BRAIN
ORIGINAL ARTICLE

DJ-1 is an essential downstream mediator in PINK1/parkin-dependent mitophagy

Dorien Imberechts,[1] Inge Kinnart,[1] Fieke Wauters,[1] Joanne Terbeek,[1] Liselot Manders,[1] Keimpe Wierda,[2] Kristel Eggermont,[3] Rodrigo Furtado Madeiro,[3] Carolyn Sue,[4] Catherine Verfaillie[3] and Wim Vandenberghe[1,5]

See Ganley (https://doi.org/10.1093/brain/awac405) for a scientific commentary on this article.

Loss-of-function mutations in the *PRKN*, *PINK1* and *PARK7* genes (encoding parkin, PINK1 and DJ-1, respectively) cause autosomal recessive forms of Parkinson's disease. PINK1 and parkin jointly mediate selective autophagy of damaged mitochondria (mitophagy), but the mechanisms by which loss of DJ-1 induces Parkinson's disease are not well understood. Here, we investigated PINK1/parkin-mediated mitophagy in cultured human fibroblasts and induced pluripotent stem cell-derived neurons with homozygous *PARK7* mutations. We found that DJ-1 is essential for PINK1/parkin-mediated mitophagy. Loss of DJ-1 did not interfere with PINK1 or parkin activation after mitochondrial depolarization but blocked mitophagy further downstream by inhibiting recruitment of the selective autophagy receptor optineurin to depolarized mitochondria. By contrast, starvation-induced, non-selective autophagy was not affected by loss of DJ-1. In wild-type fibroblasts and induced pluripotent stem cell-derived dopaminergic neurons, endogenous DJ-1 translocated to depolarized mitochondria in close proximity to optineurin. DJ-1 translocation to depolarized mitochondria was dependent on PINK1 and parkin and did not require oxidation of cysteine residue 106 of DJ-1. Overexpression of DJ-1 did not rescue the mitophagy defect of PINK1- or parkin-deficient cells. These findings position DJ-1 downstream of PINK1 and parkin in the same pathway and suggest that disruption of PINK1/parkin/DJ-1-mediated mitophagy is a common pathogenic mechanism in autosomal recessive Parkinson's disease.

1   Laboratory for Parkinson Research, KU Leuven, 3000 Leuven, Belgium
2   Electrophysiology Expertise Unit, VIB-KU Leuven Center for Brain and Disease Research, 3000 Leuven, Belgium
3   Stem Cell and Developmental Biology, KU Leuven, 3000 Leuven, Belgium
4   Department of Neurogenetics, Kolling Institute of Medical Research, Royal North Shore Hospital and University of Sydney, St. Leonards 2065, Australia
5   Department of Neurology, University Hospitals Leuven, 3000 Leuven, Belgium

Correspondence to: Wim Vandenberghe
Department of Neurology, University Hospitals Leuven
Herestraat 49, 3000 Leuven, Belgium
E-mail: wim.vandenberghe@uzleuven.be

Introduction

Parkinson's disease (PD), the fastest growing of all neurological disorders,[1] is a neurodegenerative condition characterized clinically by a wide range of disabling motor and non-motor symptoms.[2] Disease-modifying treatments for PD are still lacking. A minority of cases show a Mendelian inheritance pattern. Loss-of-function mutations in *PRKN*, *PINK1* and *PARK7* cause autosomal recessive PD, while autosomal dominant forms can be caused by *LRRK2* and *VPS35* mutations and by missense mutations or multiplications of *SNCA*.[3] In addition, multiple genes (e.g. *FBXO7*, *ATP13A2*, *VPS13C*) have been linked to atypical parkinsonism syndromes that are clinically distinct from PD.[4]

PINK1 and parkin, the gene products of *PINK1* and *PRKN*, respectively, together orchestrate mitophagy, a form of selective autophagy that specifically eliminates damaged mitochondria.[5,6,7] PINK1 is a ubiquitin kinase that is imported into healthy mitochondria and constitutively degraded. Mitochondrial damage, typically manifesting as reduced mitochondrial membrane potential, arrests mitochondrial PINK1 import and stabilizes active PINK1 on the outer mitochondrial membrane (OMM). PINK1 then phosphorylates serine 65 (Ser65) of ubiquitin that is present in small amounts on the OMM. Phospho-ubiquitin serves as the mitochondrial receptor for the E3 ubiquitin ligase parkin. After translocating from the cytosol to the OMM, parkin is itself phosphorylated by PINK1 on the homologous Ser65 residue of its ubiquitin-like domain.[5,6,7] Binding of parkin to phospho-ubiquitin in combination with parkin phosphorylation induces a conformational change in parkin, resulting in its activation as an E3 ubiquitin ligase. Active parkin then ubiquitinates a large number of OMM substrates (e.g. mitofusin 1 and 2, VDAC and Miro1), thus creating more substrate for PINK1-mediated ubiquitin phosphorylation, which in turn leads to further parkin recruitment.[5,6,7] Some of these ubiquitinated OMM substrates are extracted from the OMM and degraded by the proteasome. Proteasomal degradation of mitofusins enhances mitochondrial fission, thus isolating defective areas of the mitochondrial network, while proteasomal degradation of Miro1 arrests mitochondrial motility.[5,6,7] Mitochondrial ubiquitin chains are also recognized by the autophagy receptors optineurin and NDP52[8,9,10] (of which only optineurin is expressed in neural tissue),[8,11,12] which simultaneously bind to ubiquitin and to LC3 present on growing phagophores. Closure of the autophagosome around the damaged mitochondrion eventually allows fusion with a lysosome and degradation. Loss of function of parkin or PINK1 as a result of PD-linked mutations disrupts mitophagy, leading to accumulation of dysfunctional mitochondria and cell death.[5,6,7] Mitophagy-independent functions of PINK1 and parkin have also been described.[13,14]

PARK7 mutations are the rarest known cause of autosomal recessive PD.[15,16] Clinically, PD caused by *PARK7* mutations is indistinguishable from disease resulting from *PRKN* or *PINK1* mutations. *PARK7* encodes DJ-1, a 19.9-kDa protein whose physiological function has remained largely enigmatic despite intensive research.[17] Many different roles for DJ-1 have been reported. For example, DJ-1 has been proposed to function as a transcriptional regulator,[18] a scavenger of reactive oxygen species,[19,20] a glyoxalase,[21] a protease,[22] an aldehyde-adduct hydrolase,[23] a regulator of the 20S proteasome,[24] a chaperone for α-synuclein,[25] an adaptor for complexes involved in regulation of catecholamine homeostasis,[26] a promotor of synaptic vesicle endocytosis[27] and an RNA-binding protein,[28] but a clear picture of its molecular function has not emerged yet. DJ-1-deficient cells contain dysfunctional mitochondria, and it has been suggested that DJ-1 may control autophagy and mitochondrial homeostasis.[29,30] However, the underlying mechanisms are not clear. Here, we investigated whether DJ-1 is involved in PINK1/parkin-dependent mitophagy in human fibroblasts and neurons.

Materials and methods

Antibodies

The following primary antibodies were used for western blot (WB), immunofluorescence (IF) and proximity ligation assays (PLA): mouse anti-β-actin (WB, 1:5000; Sigma, A5441), rabbit anti-HSP60 (WB, 1:1000; IF, 1:1000; Abcam, ab53109), goat anti-HSP60 (IF, 1/500; MyBioSource, MBS423631), mouse anti-ATP5F1B (WB, 1:1000, IF, 1:500; Abcam, ab14730), mouse antimitofusin 2 (WB, 1:1000; Abcam, ab56889), mouse anti-LC3B (WB, 1:2000; Novus Biologicals, NB100-2220), rabbit anti-RAB10 (WB, 1:1000; Cell Signaling Technology, 8127S), rabbit antiphospho-RAB10^{T73} (WB, 1:500; Abcam, ab230261), rabbit anti-PINK1 (WB, 1:1000; Novus Biologicals, BC100-494), rabbit anti-optineurin (WB, 1:1000; IF, 1:200; Abcam, ab23666), mouse anti-optineurin (IF and PLA, 1:50; Santa Cruz, sc-166576), rabbit anti-DJ-1 (WB, 1:1000; IF and PLA, 1/250; Abcam, ab18257), rabbit antityrosine hydroxylase (TH) (WB, 1:500; IF, 1:500; Sigma, AB152), mouse anti-TH (IF, 1:500; Sigma, MAB318), sheep anti-TH (IF, 1:500; Thermo Fisher, PA1-4679), mouse anti-MAP2 (IF, 1:500; Sigma, M1406), mouse anti-PSD95 (IF, 1:500; Cell Signaling, 36233), rabbit antisynaptophysin (IF, 1:500; Thermo Fisher, MA5-14532), mouse anti-ubiquitin (WB, 1:50; Santa Cruz, sc-8017), rabbit antiphospho-ubiquitin^{S65} (WB, 1:1000; IF, 1:250; Sigma, ABS1513-I), mouse anti-FLAG (WB, 1:1000; IF, 1:500; Sigma, F3165), rabbit anti-FLAG (WB, 1:1000; IF, 1:500 Sigma, F7425), goat anti-FLAG (IF, 1/500; Origene, TA150080), mouse anti-GTP cyclohydrolase 1 (PLA, 1:50; Abnova, H00002643-M01), mouse antiprotein disulphide isomerase (PLA, 1:500; Enzo Life Sciences, ADI-SPA-891), mouse anti-EEA1 (PLA, 1/500; BD Biosciences, 610456), rabbit anti-calnexin (PLA, 1/500; Enzo, ADI-SPA-860), mouse anti-GM130 (PLA, 1/200; BD Biosciences, 610822), rabbit anti-GOLGA5 (PLA, 1/500; Sigma, HPA000992), mouse anti-COPB1 (WB, 1:1000; Sigma, G6160), rabbit anti-TBK1 (WB, 1:1000; Cell Signaling, 3504S), rabbit antiphospho-TBK1^{S172} (WB, 1:1000; Cell Signaling, 5483S), rabbit anti-NDP52 (WB, 1:1000; Cell Signaling, 60732S), rabbit anti-GFAP (ICC, 1:500; Agilent Dako, Z0334) and mouse anti-TOMM20 (ICC, 1:500; Santa Cruz, sc-17764). Peroxidase-linked secondary antibodies for WB were from Sigma (SAB3700934 and SAB3701095). Secondary antibodies for IF were donkey antimouse Alexa Fluor-488, −555 and −647 (Thermo Fisher, a21202, a21206, a31571), antirabbit Alexa Fluor-488, −555 and −647 (Thermo Fisher, a31570, a31572, a31573) and antisheep Alexa Fluor-488, −555 and −647 (Thermo Fisher, a11015, a21436, a21448).

cDNAs, siRNAs and lentivirus

pCMV6-Entry vectors containing cDNA for FLAG-tagged human DJ-1 and RAB10 were purchased from Origene (RC201645 and RC201464, respectively). A pCMV6-AC-GFP empty vector and pCMV6-AC-GFP vector containing cDNA for human DJ-1 were purchased from Origene (PS100010 and RG201645, respectively). The construct encoding parkin with an N-terminal FLAG tag was described previously.[31] The mito-Keima construct (mt/mKeima/pIND[SP1]) was a gift from Dr A. Miyawaki (RIKEN Brain Science Institute, Japan[32]) and the Keima construct (mKeima-Red-N1) was a gift from Dr M. Davidson (Addgene, 54597). The GFP-LC3 construct

was a gift from Dr J. Debnath (Harvard Medical School, USA). Optineurin-EGFP was a gift from Dr B. Yue (Addgene, 27052). YFP-Parkin was a gift from Dr Richard Youle (Addgene, 23955). The FLAG-tagged-DJ-1 C106A construct was generated using the QuikChange Lightning Site-Directed Mutagenesis Kit (Agilent, 210518) with the following primers: 5′-GGCCTGATAGCCGCCA TCGCAGCAGGTCCTACTGCTCTG-3′ and 5′-CAGAGCAGTAGGACCT GCTGCGATGGCGGCTATCAGGCC-3′. Mutagenesis was verified by sequencing. To generate OMM-targeted DJ-1-FLAG (OMM-DJ-1-FLAG), the coding sequence for the N-terminal 49 amino acids of TOMM20 (gBlock purchased from IDT) was inserted into the *Bam*HI/*Sgf*I sites of the pCMV6-Entry vector containing cDNA for human DJ-1-FLAG using Gibson Assembly (NEB, E2611S). The sequence of the gBlock was: CGGCCGGGAATTCGTCGACTGAT GGTGGGTCGGAACAGCGCCATCGCCGCCGGTGTATGCGGGGCCCTT TTCATTGGGTACTGCATCTACTTCGACCGCAAAAGACGAAGTGACC CCAACTTCAAGAACAGGCTTCGAGAACGAAGAAAGAAACAGAAGC TTGCCAAGGGTGGTGGAGGCAGTGGAGGTGGAGGAAGCGGAGGTGG TGGCAGCATCGCCATGGCTTCCAAAAGAGC. *DJ-1* siRNA1 was from Santa Cruz (sc-37080) and is a pool of three siRNAs with the following target sequences: 5′-CTCCACTTGTTCTTAAAGA-3′, 5′-CGACGAT CACTTAGAGAAA-3′ and 5′-GGAAGTATGGAAGTCACAA-3′. The target sequence of *DJ-1* siRNA2 (Thermo Fisher, S22304) was 5′-GGTTTTGGAAGTAAAGTTATT-3′. The target sequence of *OPTN* siRNA1 (Thermo Fisher, S19720) was 5′-GACTTGAAGTTGCA CTCAATT-3′. *OPTN* siRNA2 was from Santa Cruz (sc-39054) and is a pool of three siRNAs with the following target sequences: 5′-CCAAGAATTACTTCGAACATT-3′, 5′-CCATCAGAGTTGAATGA AATT-3′ and 5′-GTAGAATCCTTACCTACTATT-3′. The target sequence of control siRNA (Qiagen) was 5′-AATTCTCCGAA CGTGTCACGT-3′. pLenti-C-mGFP-P2A-Puro lentiviral particles encoding human DJ-1 and lentiviral pLenti-C-mGFP-P2A-Puro control particles were purchased from Origene (RC201645L4V and PS100093V, respectively). Keima and mito-Keima DNA were cloned into the XbaI and BamHI sites of the PCDH-CMV-MCS-EF1-PURO lentiviral transfer vector (Addgene, 46970), followed by production of lentiviral particles by cotransfecting human embryonic kidney 293T cells with packaging plasmids psPAX2 (Addgene, 12260) and pMD2.G (Addgene, 12259) and with PCDH-CMV-MCS-EF1-PURO lentiviral transfer vector (Addgene, 46970) containing mito-Keima or Keima DNA using X-treme GENE™ 9 DNA Transfection Reagent (Sigma, 6365809001). After 12 h, transfection medium was changed with fresh medium [DMEM (Thermo Fisher, 41965) supplemented with foetal bovine serum (10%; Greiner Bio-One, 10270106), penicillin (100 U/ml; Thermo Fisher, 15140112), streptomycin (100 µg/ml; Thermo Fisher, 15140112) and sodium pyruvate (1 mM; Thermo Fisher, 11360070)] and recombinant lentiviruses were harvested 72 h after transfection. The culture medium containing virus particles was collected and filtered through 0.45-µm polyvinyl difluoride membrane filters (Merck, SLHV033R). Particles were concentrated with a filter device (Amicon Ultra-15 Centrifuge Filters, Merck, UFC910096), aliquoted and stored at −80°C.

Cultures of fibroblasts from Parkinson's disease patients and healthy controls

Fibroblasts were obtained from PD patients and age-matched healthy controls via skin biopsy from the medial aspect of the upper limb after written informed consent. All procedures were approved by the local ethics committee and were in accordance with the latest version of the World Medical Association Declaration of Helsinki. The clinical history of the PD patient with homozygous

PARK7 mutations has been described.[33] The PD patient with compound heterozygous *PRKN* mutations (deletion of exon 2 and duplication of exon 6) was a female who developed rest tremor of the upper limbs at the age of 39 years. She had no significant non-motor symptoms. Clinical exam at the age of 41 showed mild bilateral hypokinesia, rigidity and rest tremor with left-sided predominance. Brain MRI was normal. ^{123}I-FP-CIT SPECT showed severely, symmetrically reduced uptake in the putamina and to a lesser extent the caudate nuclei. She had an excellent response to pramipexole. Disease progression was very slow. After 11 years of disease progression, she was still on monotherapy with pramipexole extended release 3.15 mg q.d. Skin biopsy was obtained at the age of 46. The clinical history of the PD patient with homozygous W437G mutations in *PINK1* was described before.[34] Healthy controls included a 40-year-old female (Ctrl1) and a 28-year-old male (Ctrl2), who both had a normal clinical neurological exam. Fibroblasts were cultured as described[35] in DMEM F12 (Invitrogen, 31331093) supplemented with foetal bovine serum (10%; Greiner Bio-One, 10270106), non-essential amino acids (1%; Thermo Fisher, 11140035), penicillin (100 U/ml; Thermo Fisher, 15140112), streptomycin (100 µg/ml; Thermo Fisher, 15140112) and sodium bicarbonate (0.12%; Sigma, S8761) at 37°C in a 5% CO_2 humidified atmosphere. Cultures were repeatedly tested for *Mycoplasma* and tests were always negative. Fibroblast experiments were performed at passage numbers 5–14. Within the same experiment, control and mutant fibroblasts were used at similar passage numbers.

iPSC generation

Fibroblasts from the PD patient with *PARK7* mutations, the PD patient with *PRKN* mutations and healthy control Ctrl1 were reprogrammed to induced pluripotent stem cells (iPSCs) via Sendai virus-mediated overexpression of Yamanaka transcription factors *OCT4*, *SOX2*, *KLF4* and *C-MYC*.[36] Three iPSC clones were generated per patient and checked for clearance of the Sendai virus. All iPSC clones underwent state-of-the-art quality controls: immunofluorescent staining for pluripotency markers, analysis of expression of self-renewal genes and trilineage differentiation potential, SNP analysis to confirm genomic identity with the initial fibroblasts and array comparative genomic hybridization to exclude chromosomal defects (Supplementary Methods; Supplementary Figs 1–5). A second healthy control iPSC line from a 24-year-old female (Ctrl3) was obtained from Sigma (IPSC0028).

Differentiation of iPSCs to dopaminergic neurons

iPSCs were expanded until confluent on Matrigel (VWR, BDAA356277)-coated six-well plates (VWR, 734–2323) in mTeSR basal medium supplemented with mTeSR 5× supplement (StemCell Technologies, 85850), penicillin (10 U/ml; Thermo Fisher, 15140112) and streptomycin (10 µg/ml; Thermo Fisher, 15140112). For splitting, cells were washed briefly with PBS, incubated with ReLeSR (Stemcell Technologies, 5873) at room temperature for 4 min, collected in mTeSR medium and seeded. iPSCs were differentiated to dopaminergic neurons as described.[37] To dissociate cells, iPSCs were incubated with 1 ml/well accutase (400–600 U/ml, Sigma, A6964) for 4 min at 37°C. Cells were suspended in accutase and the plate was rinsed with 2 ml/well of mTeSR to collect remaining cells. After centrifugation for 5 min at 300*g*, supernatant was discarded and cells were resuspended in mTeSR containing 2 µl/ml Y-27632 ROCK inhibitor (Sigma, 688001) and seeded on

Matrigel-coated six-well plates. To induce neuronal differentiation, medium was switched on the next day (day 0 of induction) to KSR [KnockOut DMEM medium (Life Technologies, 10829018) containing 15% KnockOut Serum Replacement (Life Technologies, 10828010), 2 mM L-glutamine, 10 mM β-mercaptoethanol, 1% non-essential amino acids, 10 U/ml penicillin and 10 µg/ml streptomycin] supplemented with LDN-193189 (100 nM, Miltenyi Biotec, 130-106-540) and SB-431542 (10 µM, R&D systems, 1614). Medium was replaced on day 1 by KSR supplemented with LDN-193189 (100 nM), SB-431542 (10 µM), FGF8b (100 ng/ml, R&D systems, 423-F8), SHH (C25II) (100 ng/ml, R&D systems, 464-SH) and purmorphamine (2 µM, Merck Millipore, 540223). On day 3, CHIR-99021 (3 µM, Tocris, 4423) was added. From day 5 onwards, KSR medium was gradually shifted (¼ NB + ¾ KSR on day 5, ½ NB + ½ KSR on day 7, ¾ NB + ¼ KSR on day 9) to NB medium [Neurobasal medium (Life Technologies, 21103049) supplemented with B27 (Life Technologies, 12587010) and N2 (Life Technologies, 17502048), 2 mM L-glutamine, 10 U/ml penicillin and 10 µg/ml streptomycin]. On day 11, medium was completely replaced by NB medium containing CHIR-99021 (3 µM), BDNF (20 ng/ml, Peprotech, AF-450–02), ascorbic acid (0.2 mM, A4544, Sigma), GDNF (20 ng/ml, Peprotech, AF-450-10), TGFβ3 (1 ng/ml, Peprotech, 100-36E), dibutyryl cAMP (0.5 mM, Sigma, D0627) and DAPT (10 µM, Tocris, 2634). On day 13, cells were dissociated using accutase and replated 1:1 on Matrigel-coated plates in differentiation medium (same composition as day 11 NB medium but without CHIR-99021) and medium was replaced every other day. On day 20, cells were dissociated again using accutase and replated at high cell density (±15 000 cells/well for a 12-well plate, ± 350 000 cells/well for a six-well plate) on plates precoated with poly-L-ornithine (50 µg/ml, Sigma, P3655) and laminin (10 µg/ml, Sigma, L2020) and maintained in differentiation medium until day 50 by replacing medium three times a week. Once a week, the fresh medium contained 10 µg/ml laminin. HeLa cells (for comparison of autophagy receptor expression levels with fibroblasts and iPSC-derived neurons) were cultured as described.[31]

Transfection and lentiviral transduction

Fibroblasts were transiently transfected with 50 nM siRNA or 0.3 µg/µl cDNA (final concentrations) using the Neon Transfection System (Invitrogen, MPK1096) according to the manufacturer's instructions. Neurons were transduced with lentivirus on day 48–50 after neuronal induction.

Western blot, mitochondrial isolation and coimmunoprecipitation

WB was performed as described.[35] In brief, cells were washed with ice-cold PBS, removed with a scraper and resuspended in PBS (350 mM NaCl, 2.7 mM KCl, 10.2 mM Na$_2$PO$_4$, 1.75 mM KH$_2$PO$_4$, pH 7.4) with 1% Triton X-100 (Sigma, 93443). After solubilization on ice for 30 min, insoluble material was removed by centrifugation at 20 000g for 5 min. Protein concentrations were determined using Bio-Rad Protein assay. Sodium dodecyl-sulphate loading dye was added to the samples, followed by denaturation at 99°C for 10 min, sodium dodecyl-sulphate–polyacrylamide gel electrophoresis, blotting onto polyvinyl difluoride membranes and incubation with blocking solution, primary and secondary antibodies. Immunoreaction was visualized with Luminata Classico (Thermo Fisher, wbluc0100) or Amersham ECL Select (VWR, RPN2235) on a Fujifilm LAS-3000 Imager. The density of scanned signals was measured with UN-SCAN-IT gel 7.1 (Silk Scientific). Mitochondria were isolated as previously described.[34] For coimmunoprecipitation, fibroblasts transfected with FLAG-tagged DJ-1 were washed with ice-cold PBS, removed with a scraper and resuspended in lysis buffer (20 mM Tris-HCl, 500 mM NaCl and 1% Triton X-100, pH 7.4). After solubilization for 30 min at 4°C, insoluble material was removed by centrifugation at 20 000g for 5 min. Equal protein amounts were incubated with anti-FLAG M2 Affinity Gel (Sigma, A2220) for 2 h at 4°C after which beads were washed three times with lysis buffer. Bound proteins were eluted in lysis buffer containing FLAG peptides (0.1 µg/µl; Sigma, F3290) for 30 min at 4°C, followed by WB.

Immunofluorescence, confocal microscopy and image analysis

Immunostaining of cultured cells was performed as described.[35] TOTO-3 for nuclear staining was purchased from Thermo Fisher (T3604). Confocal images with 0.5 µm slice thicknesses were acquired at room temperature with a Leica TCS SP5 II confocal microscope equipped with a ×63 or ×100 objective lens (HC PL APO ×63 or ×100/1.4 CS2), a multi-argon laser (458, 476, 488 nm) and a He/Ne laser (543 nm). Random images were captured and analysed by an investigator blinded to genotype and experimental condition. A minimum of 200 cells per condition was analysed per experiment.

Structured illumination microscopy

Cells were grown on 1.5H High Performance coverslips (Marienfeld). Coverslips were mounted with ProLong Glass Antifade Mountant (P36984, Thermo Fisher). For image acquisition, a Nikon Ti2 N-structured illumination microscopy (SIM) S microscope equipped with a Hamamatsu ORCA-Flash 4.0 [(C13440) slow, no binning] was used in combination with a ×100 SR Apo TIRF AC objective lens (NA 1.49). The setup was controlled by NIS-Elements 5.21.02 (build 1487). 0.5 µm z-stacks were acquired in 3D-SIM mode (0.03 µm steps) at room temperature. Alexa 488 fluorophore was excited at 488 nm and collected at 525/30. Alexa 555 fluorophore was excited at 543 nm and collected at 595/30. Alexa 647 fluorophore was excited at 633 nm and collected at 720/100 in widefield mode to check for TH- or FLAG-positive cells. Image visualization was done using Arivis vision x54, v.3.3 (Arivis AG). NIS-Elements AR 5.40 (Nikon) was used to analyse 3D-SIM stacks. The analysis of the images included background subtraction by constant, thresholds in 3D and measurement of overlapping volumes and total volumes. All conditions were processed in batch. Ten cells per condition were analysed per experiment.

Proximity ligation assay

Cells were fixed and permeabilized as described for immunostaining. Antibody incubation and probe amplification were performed according to the manufacturer's instructions (Duolink *In Situ* Red Starter Kit Mouse/Rabbit, Sigma, DUO 92101). For combination of PLA with immunostaining of mitochondria, cells were incubated simultaneously with goat anti-HSP60 antibody and primary antibodies used for PLA. Following the washing steps, cells were incubated with secondary antibody for immunofluorescence together with the PLA probes. Samples were covered with the Duolink detection solution, washed and mounted according to the PLA protocol. Confocal images with 0.5-µm slice thicknesses were acquired at room temperature with a Leica TCS SP5 II confocal microscope and analysed as described before.

Electrophysiology

Neurons were initially whole-cell voltage clamped at −70 mV using a double EPC-10 amplifier (HEKA Elektronik, Lambrecht/Pfalz, Germany) under the control of Patchmaster v.2x32 software (HEKA Elektronik). The intracellular pipette solution contained (in mM): 136 KCl, 18 HEPES, 4 Na-ATP, 4.6 $MgCl_2$, 4 K2-ATP, 15 creatine phosphate, 1 EGTA and 50 U/ml phosphocreatine kinase (300 mOsm, pH 7.30). The extracellular solution contained (in mM): 140 NaCl, 2.4 KCl, 2 $CaCl_2$, 2 $MgCl_2$, 10 HEPES, 14 glucose (300 mOsm, pH 7.30). Currents were recorded at 20 Hz and low-pass filtered at 3 kHz when stored. Pipettes were pulled using a Sutter P-1000 and resistance ranged from 3 to 5 MΩ. The series resistance was compensated to 70–75%. Cells with series resistances above 15 MΩ were excluded. Spontaneous synaptic events were recorded in whole-cell voltage clamp configuration [holding potential ($V_{holding}$) = −70 mV]. Resting membrane potential V_{rest} and endogenous firing activity were measured in current clamp ($I_{holding}$ = 0 pA). Recordings were performed at room temperature.

Live mito-Keima and Keima imaging

Fibroblasts were transiently transfected with mito-Keima or Keima cDNA. When cotransfecting fibroblasts with mito-Keima and FLAG-tagged DJ-1, a 1:3 molar ratio for mito-Keima cDNA relative to FLAG-DJ-1 cDNA was used, and immunostaining showed that all mito-Keima-positive cells were also FLAG-positive under these conditions (not shown). Neurons were transduced on day 48 after neuronal induction with lentivirus containing mito-Keima or Keima. Cells were treated with valinomycin, oligomycin, antimycin A, 3-methyladenine, Mito-TEMPO (Sigma, V3639, 495455, A8674, M9281, SML0737), bafilomycin A1 (Abcam, ab120497), PF-064475 and MLi-2 (Tocris, 5716, 5756) and Torin1 (Tocris, 4247). Starvation-induced autophagy was triggered by incubation in Earle's balanced salt solution (EBSS) (Sigma, E2888). For live mito-Keima or Keima imaging, random images were captured and analysed by an investigator blinded to genotype and experimental condition. Images were analysed on the Leica TCS SP5 II confocal microscope with ×63 objective lens described previously. Keima and mito-Keima were imaged in two channels via two sequential excitations (458 nm, green; 543 nm, red) and using a 600- to 695-nm emission range. Ratio (543:458) images were created using the Ratio Plus plugin in ImageJ, and high (543:458) ratio areas were segmented. The parameter [high (543:458) ratio area:total cell area] was used as an index of autophagy and the parameter [high (543:458) ratio area:total mitochondrial area] as an index of mitophagy, as described.[32,35] Approximately 15 cells were analysed per condition per experiment, and at least 10 z-stacks with 0.5-μm slice thicknesses were acquired per cell.

Statistics

The significance of differences was analysed with two-tailed Student's *t*-test for comparison between two groups and with one-way ANOVA and *post hoc* Tukey's test for comparison between more than two groups (GraphPad prism 9, GraphPad Software, Inc.). Data were presented as mean ± SEM. A P-value of <0.05 was considered statistically significant.

Data availability

The data that support the findings of this study are available from the corresponding author upon reasonable request.

Results

Mitophagy is impaired in DJ-1-deficient human skin fibroblasts

We recently identified a homozygous *PARK7* mutation (c.471_473delGCC; p.Pro158del) in a 30-year-old man with juvenile PD.[33] DJ-1 protein levels in cultured skin fibroblasts from this patient were only 3.8 ± 1.1% (P < 0.001; n = 3) and 4.5 ± 1.5% (P < 0.001; n = 3) of the levels in fibroblasts from a 40-year-old female healthy control (Ctrl1) and a 28-year-old male healthy control (Ctrl2), respectively (Fig. 1A). This is consistent with previous work showing that the Pro158 deletion drastically impairs the stability of DJ-1.[38]

To induce mitophagy we exposed the fibroblasts to the mitochondrial uncoupler valinomycin. We previously showed that valinomycin-induced mitophagy in human skin fibroblasts is PINK1- and parkin-dependent.[34,35] We first used live mito-Keima imaging to measure mitophagic flux.[35] Mito-Keima is a mitochondrially targeted form of Keima, a fluorescent protein that is resistant to lysosomal proteases and exhibits pH-dependent excitation.[32] The peak of the excitation spectrum of mito-Keima shifts when mitochondria are delivered to acidic lysosomes, allowing live dual-excitation ratiometric quantification of mitophagy.[32] In fibroblasts from healthy controls, mito-Keima imaging showed that valinomycin-induced mitophagy, which was suppressed by the lysosomal vacuolar-type H^+-ATPase inhibitor bafilomycin A1, consistent with previous work [35] (Fig. 1B and C). Interestingly, valinomycin-induced mitophagy was severely suppressed in *PARK7* mutant fibroblasts, to a similar extent as in cells from PD patients with compound heterozygous *PRKN* or homozygous *PINK1* mutations (Fig. 1B and C). We confirmed the mitophagy defect in the *PARK7* mutant fibroblasts by measurement of valinomycin-induced clearance of the mitochondrial matrix protein HSP60 by WB (Fig. 1D and E) and immunostaining (Fig. 1F and G). The mitophagy defect of *PARK7* mutant fibroblasts was rescued by overexpression of wild-type DJ-1 (Fig. 1H–J). Finally, knockdown of DJ-1 in control fibroblasts with two different siRNAs also suppressed mitophagy (Fig. 1K–M and Supplementary Fig. 6).

Taken together, these data indicated that valinomycin-induced mitophagy in human fibroblasts requires DJ-1.

Previous work has shown that cysteine residue 106 (C106) of DJ-1 is highly sensitive to oxidation by H_2O_2 and that C106 oxidation is required for some of the cellular effects of DJ-1.[20,39] We generated a DJ-1 construct in which C106 was replaced by alanine (C106A). DJ-1^C106A rescued mitophagy in *PARK7* mutant fibroblasts as efficiently as wild-type DJ-1 (Fig. 1H–J), indicating that the function of DJ-1 in mitophagy did not require C106 oxidation.

DJ-1 has been reported to protect against oxidative stress.[19,20] We tested whether Mito-TEMPO, a scavenger of reactive oxygen species (ROS), could rescue the mitophagy defect of *PARK7* mutant fibroblasts, but this was not the case (Supplementary Fig. 7), suggesting that the mitophagy defect of the mutant cells was not caused by oxidative stress.

Mitophagy is impaired in DJ-1-deficient iPSC-derived human neurons

We reprogrammed the *PARK7* mutant, *PRKN* mutant and Ctrl1 fibroblasts to iPSCs. We differentiated two iPSC clones from the *PARK7* patient, two iPSC clones from the *PRKN* patient, one iPSC clone from Ctrl1 and a commercially available iPSC clone from a healthy 24-year-old female (Ctrl3) to dopaminergic neurons. This yielded cultures in which ~80% of all cells on day 50 after neuronal induction were neurons based on labelling for the neuronal marker MAP2 and ~55% of all cells were dopaminergic based on staining
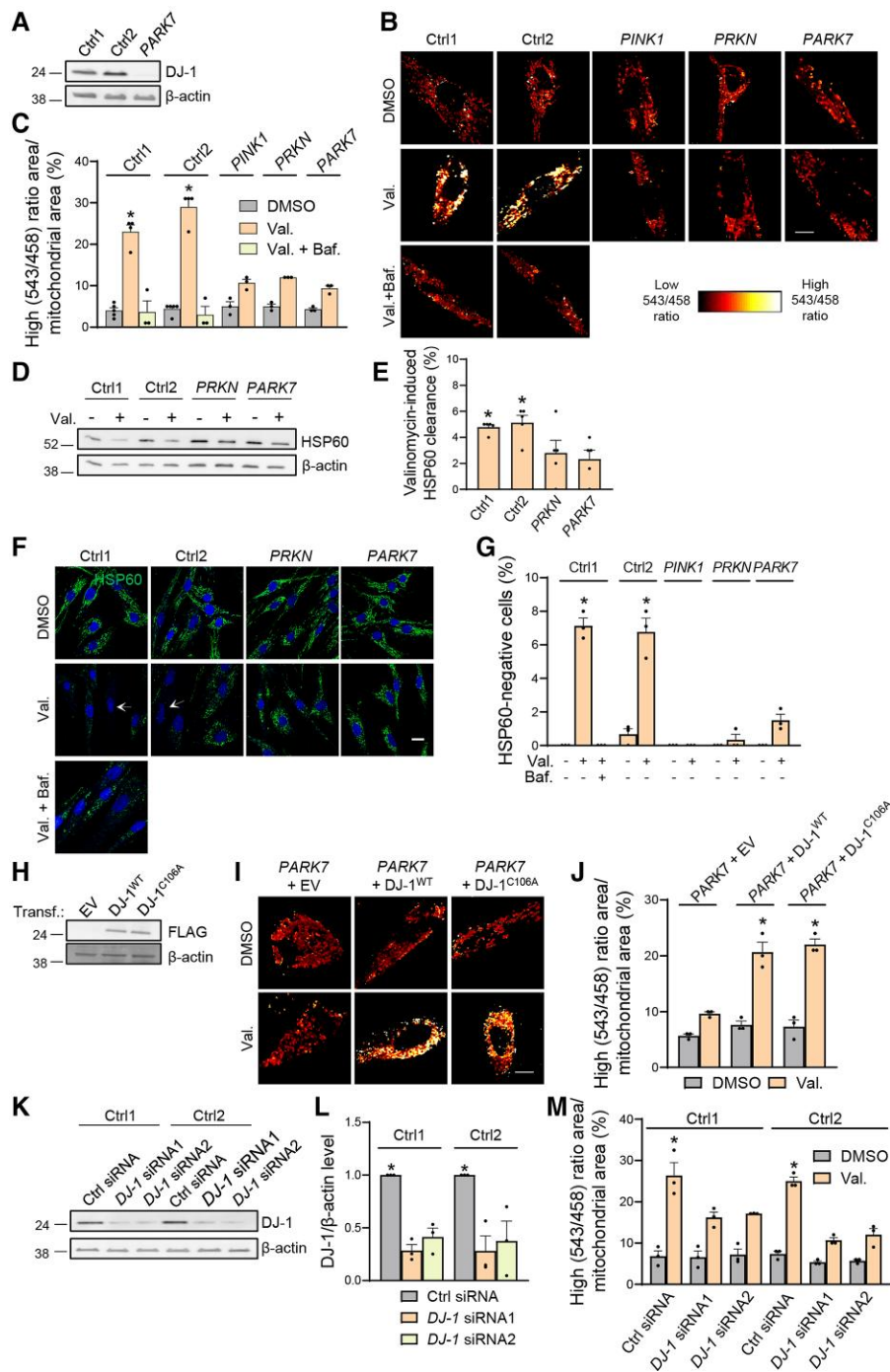
Figure 1 Impaired mitophagy in DJ-1-deficient human fibroblasts. (**A**) WB for endogenous DJ-1 in fibroblasts from healthy controls (Ctrl1, Ctrl2) and a PD patient with homozygous *PARK7* mutations. (**B** and **C**) Fibroblasts from healthy controls and PD patients with homozygous *PINK1,* compound heterozygous *PRKN* and homozygous *PARK7* mutations were transfected with mito-Keima and treated for 48 h with DMSO, valinomycin (Val., 1 μM) and bafilomycin A1 (Baf., 100 nM), followed by live ratiometric imaging. High (543:458) ratio signal corresponds to mito-Keima present in lysosomes. (**C**) High (543:458) ratio area/total mitochondrial area was quantified as an index of mitophagy (n = 3–5). *$P < 0.001$ compared with all conditions other than Ctrl Val. (**D** and **E**) Fibroblasts from healthy controls and patients with *PRKN* or *PARK7* mutations were treated for 48 h with DMSO or Val., followed by western. (**E**) Quantification (n = 5). *$P < 0.05$ compared with *PRKN* and *PARK7*. (**F** and **G**) Fibroblasts were treated as indicated for 48 h and immunostained for mitochondrial marker HSP60. Nuclei were stained with TOTO-3. Arrows indicate examples of cells without detectable HSP60 staining. (**G**) Quantification of percentage cells without detectable HSP60 (n = 3, with at least 200 cells analysed per condition in each of the three experiments). *$P < 0.0001$ compared with all conditions other than Ctrl Val. (**H**) WB of Ctrl1 fibroblasts transfected with empty vector (EV) or FLAG-tagged wild-type (WT) or C106A DJ-1. (**I** and **J**) *PARK7* mutant fibroblasts were cotransfected with mito-Keima and either EV or FLAG-tagged WT or C106A DJ-1. After 24 h, cells were treated with DMSO or Val. (1 μM) for 48 h, followed by mito-Keima imaging. (**J**) Quantification (n = 3). *$P < 0.0001$ compared with EV Val. and all DMSO conditions. (**K** and **L**) Control fibroblasts were transfected with the indicated siRNAs for 72 h, followed by western. (**L**) Quantification (n = 3). *$P < 0.05$ compared with all other conditions in the same subject. (**M**) Control fibroblasts were transfected with mito-Keima and the indicated siRNAs. After 72 h, cells were treated with DMSO or Val. (1 μM) for 48 h, followed by mito-Keima imaging and quantification (n = 3). *$P < 0.005$ compared with all other conditions in the same subject. Scale bars = 10 μm. Illustrations of mito-Keima imaging in the siRNA-transfected cells are shown in Supplementary Fig. 6.
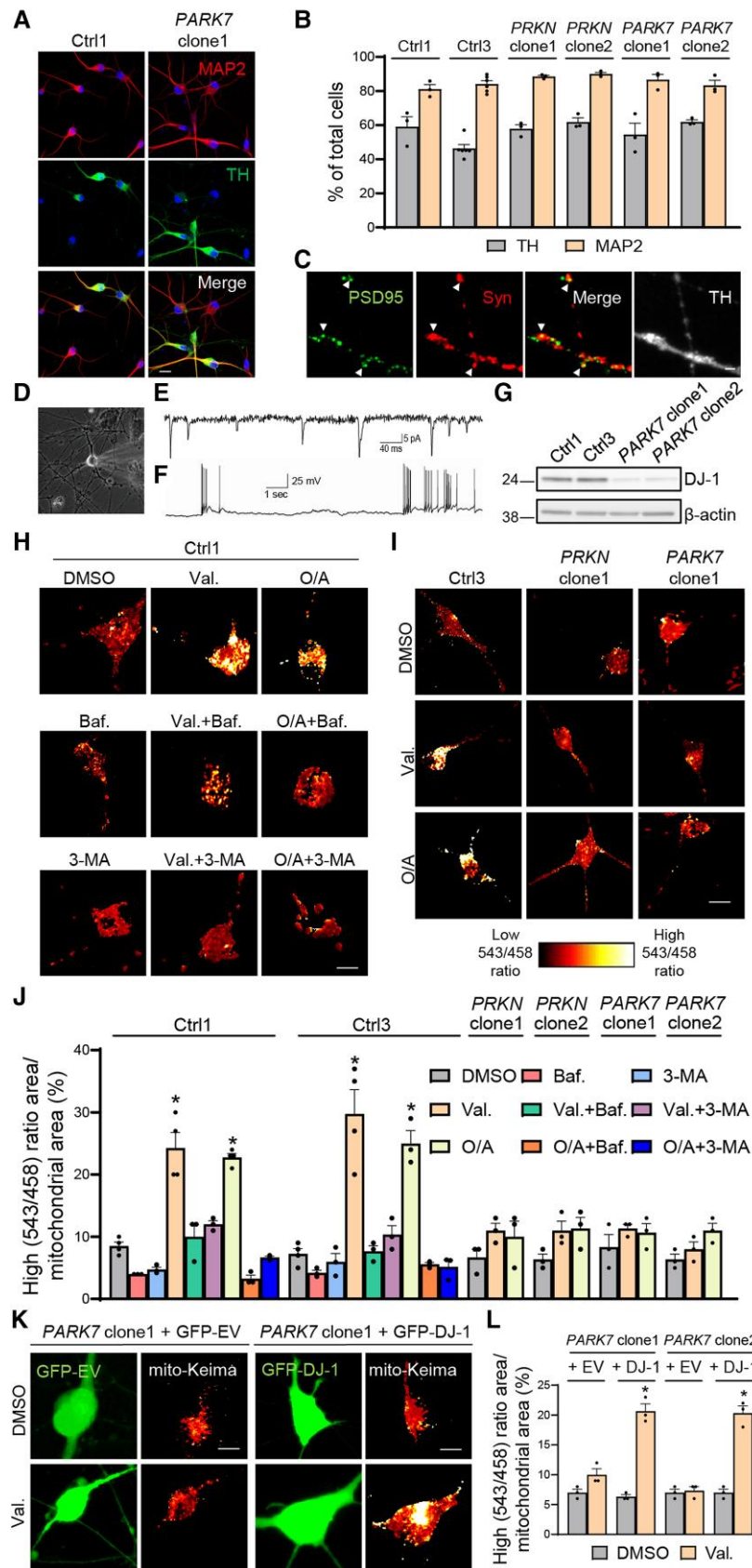
Figure 2 Impaired mitophagy in DJ-1-deficient iPSC-derived human neurons. (A and B) On Day 50 after neuronal induction, iPSC-derived neuronal cultures from healthy controls (Ctrl1, Ctrl3) and PD patients with *PRKN* (clones 1 and 2) and *PARK7* mutations (clones 1 and 2) were immunostained for MAP2 and tyrosine hydroxylase (TH). Nuclei were stained with TOTO-3. Scale bar = 20 μm. TH and MAP2 immunostainings of neuronal cultures derived from Ctrl3, *PRKN* mutant (clones 1 and 2) and *PARK7* mutant (clone 2) iPSCs are shown in Supplementary Fig. 8. **(B)**

(Continued)

for TH (Fig. 2A and B and Supplementary Fig. 8). These percentages were not significantly different between control, *PARK7* and *PRKN* cultures (Fig. 2B). Percentages of GFAP-positive cells (astrocytes) on day 50 after neuronal induction were $2.0 \pm 0.5\%$ in Ctrl1 cultures, $2.9 \pm 0.6\%$ in Ctrl2 cultures, $3.0 \pm 0.8\%$ in *PRKN* mutant (clone 1) cultures and $2.0 \pm 0.6\%$ in *PARK7* mutant (clone 1) cultures ($P = 0.54$; $n = 3$). The iPSC-derived neurons formed synapses, as shown by colocalization of the presynaptic marker synaptophysin and the postsynaptic marker PSD-95 (Fig. 2C) and recording of spontaneous excitatory postsynaptic currents (Fig. 2D and E), and generated spontaneous action potentials, confirming their neuronal identity (Fig. 2F). As in the *PARK7* mutant fibroblasts, DJ-1 protein levels were nearly undetectable in the *PARK7* neurons (Fig. 2G). DJ-1 protein levels in neurons derived from *PARK7* iPSC clone 1 were only $11.3 \pm 1.2\%$ ($P < 0.01$; $n = 3$) and $9.8 \pm 0.7\%$ ($P < 0.01$; $n = 3$) of the levels in Ctrl1 and Ctrl3, respectively. DJ-1 levels in neurons from *PARK7* iPSC clone 2 were $11.8 \pm 1.2\%$ ($P < 0.01$; $n = 3$) and $8.5 \pm 1.2\%$ ($P < 0.01$; $n = 3$) of the levels in Ctrl1 and Ctrl3, respectively.

We used lentiviral transduction to express mito-Keima in the iPSC-derived neurons. To depolarize mitochondria, we exposed neurons to the electron transport chain complex III inhibitor antimycin A in combination with the ATP synthase inhibitor oligomycin, which prevents mitochondrial repolarization, or to valinomycin. In wild-type neurons, this induced substantial mitophagy, which was suppressed by bafilomycin A1 and by 3-methyladenine, an inhibitor of macro-autophagy induction (Fig. 2H–J). Importantly, mitophagy was abrogated both in *PRKN* and *PARK7* mutant neurons (Fig. 2I and J). As in the fibroblasts, overexpression of wild-type DJ-1 in *PARK7* mutant neurons restored mitophagy (Fig. 2K and L).

DJ-1 is dispensable for non-selective autophagy

Mitophagy is a form of selective autophagy in which autophagy receptors, such as optineurin, link ubiquitinated cargo to LC3 that is present on autophagosomal membranes. In addition to selective autophagy, cells are also capable of non-selective (bulk) autophagy in which cytosolic components and organelles are degraded indiscriminately via mechanisms that are independent of autophagy receptors.[40] To assess whether DJ-1 was also required for non-selective autophagy, we transfected fibroblasts with Keima (the same probe as used for mitophagy imaging except that it lacked the mitochondrial targeting sequence[32,35]) and exposed fibroblasts to amino acid starvation, a classical trigger for non-selective autophagy. There was no significant difference in starvation-induced autophagy between wild-type, *PARK7*, *PINK1* and *PRKN* mutant fibroblasts (Fig. 3A and B), suggesting that non-selective autophagy occurs independently of DJ-1, PINK1 and parkin. Measurement of lipidated LC3 (LC3-II):β-actin ratios on WB

also showed no difference in starvation-induced autophagy between control and DJ-1-deficient fibroblasts (Fig. 3C and D).

We also performed live Keima imaging in control and *PARK7* mutant iPSC-derived neurons. Basal autophagy levels were high and similar in control and *PARK7* neurons, and were significantly suppressed by bafilomycin A1 and 3-methyladenine (Fig. 3E and F). In contrast to fibroblasts, amino acid starvation did not further upregulate autophagy in neurons, consistent with previous findings in cultured mouse hippocampal neurons.[41] As an alternative way to augment non-selective autophagy, we treated the neurons for 24 h with Torin1, a potent inhibitor of the negative autophagy regulators mTORC1 and mTORC2. Torin1 also failed to significantly upregulate autophagy in control and *PARK7* neurons, in line with previous work in neurons.[41]

Collectively, these findings showed that DJ-1 is required for PINK1/parkin-mediated mitophagy, but not for starvation-induced non-selective autophagy.

Optineurin recruitment to mitochondria is impaired in DJ-1-deficient fibroblasts and neurons

We then interrogated the sequential steps of PINK1/parkin-mediated mitophagy in *PARK7* mutant cells to determine which step was disrupted. Valinomycin-induced accumulation of endogenous PINK1 was intact in *PARK7* mutant fibroblasts (Fig. 4A and B) and neurons (Fig. 4C and D). Next, we assessed PINK1-mediated ubiquitin phosphorylation. In *PINK1* mutant cells, phospho-ubiquitin formation was completely abolished, as expected (Fig. 4E, F, I and J). In *PRKN* mutant cells, phospho-ubiquitin formation on depolarized mitochondria was detectable but severely reduced compared with control cells (Fig. 4I–L), probably because loss of parkin-mediated ubiquitin chain formation on mitochondria resulted in reduced amounts of substrate for PINK1-mediated ubiquitin phosphorylation.[5,6,7,12] By contrast, *PARK7* mutant fibroblasts and dopaminergic neurons showed fully preserved phospho-ubiquitin formation and accumulation on depolarized mitochondria (Fig. 4E–L). Translocation of parkin to depolarized mitochondria (Fig. 5A and B) and ubiquitination and degradation of mitofusin 2, a substrate of parkin on the OMM, also occurred normally in *PARK7* mutant cells (Fig. 5C and D). Thus, DJ-1 was not required for the enzymatic activity of PINK1 or parkin.

However, recruitment of the autophagy receptor optineurin to damaged mitochondria was severely impaired in *PARK7* mutant fibroblasts (Fig. 6A and C and Supplementary Fig. 9A) and dopaminergic neurons (Fig. 6D and E), to a similar degree as in *PINK1* and *PRKN* mutant cells, as shown by immunostaining and confocal microscopy. Super-resolution microscopy (SIM) confirmed colocalization of endogenous optineurin with mitochondria in valinomycin-treated control, but not *PARK7* mutant, dopaminergic

---

Figure 2 Continued

Quantification of percentage of TH- and MAP2-positive cells ($n = 3$–6). (**C**) Immunostaining for PSD-95, synaptophysin (Syn) and TH in neurites from Ctrl3. Arrows indicate colocalization of PSD-95 and Syn. Scale bar = 2 μm. (**D**) Phase contrast image of iPSC-derived neuron (Ctrl3) during patch-clamp recording. (**E**) Whole-cell voltage clamp recording of iPSC-derived neuron (Ctrl3) showing spontaneous excitatory postsynaptic currents ($V_{holding} = -70$ mV). (**F**) Current-clamp recording of iPSC-derived neuron (Ctrl3) showing spontaneous action potentials and irregular bursting behaviour. $V_{rest} = -64$ mV. (**G**) WB for endogenous DJ-1 in iPSC-derived neuronal cultures from healthy controls and PD patient with *PARK7* mutations (clones 1 and 2). (**H–J**) On Day 48 after neuronal induction, neurons from healthy controls and PD patients with *PRKN* (clones 1 and 2) and *PARK7* mutations (clones 1 and 2) were transduced with mito-Keima lentivirus. After 48 h, cells were treated for 24 h with DMSO, valinomycin (Val., 1 μM), a combination of oligomycin (10 μM) and antimycin (4 μM) (O/A), bafilomycin A₁ (Baf., 100 nM) or 3-methyladenine (3-MA, 10 mM), as indicated, followed by live ratiometric mito-Keima imaging. Scale bar = 10 μm. (**J**) High (543:458) ratio area:total mitochondrial area was quantified as an index of mitophagy ($n = 3$–4). *$P < 0.005$ compared with all conditions other than Ctrl Val. and Ctrl O/A. (**K** and **L**) On day 46 after neuronal induction, *PARK7* mutant neurons (clones 1 and 2) were transduced with either GFP-tagged empty vector (EV) or GFP-tagged WT *DJ-1* lentivirus. On day 48, cells were transduced with mito-Keima lentivirus. After 24 h, cells were treated as indicated for 24 h, followed by mito-Keima imaging. Scale bar = 10 μm. (**L**) Quantification ($n = 3$). *$P < 0.0001$ compared with all other conditions in the same clone.
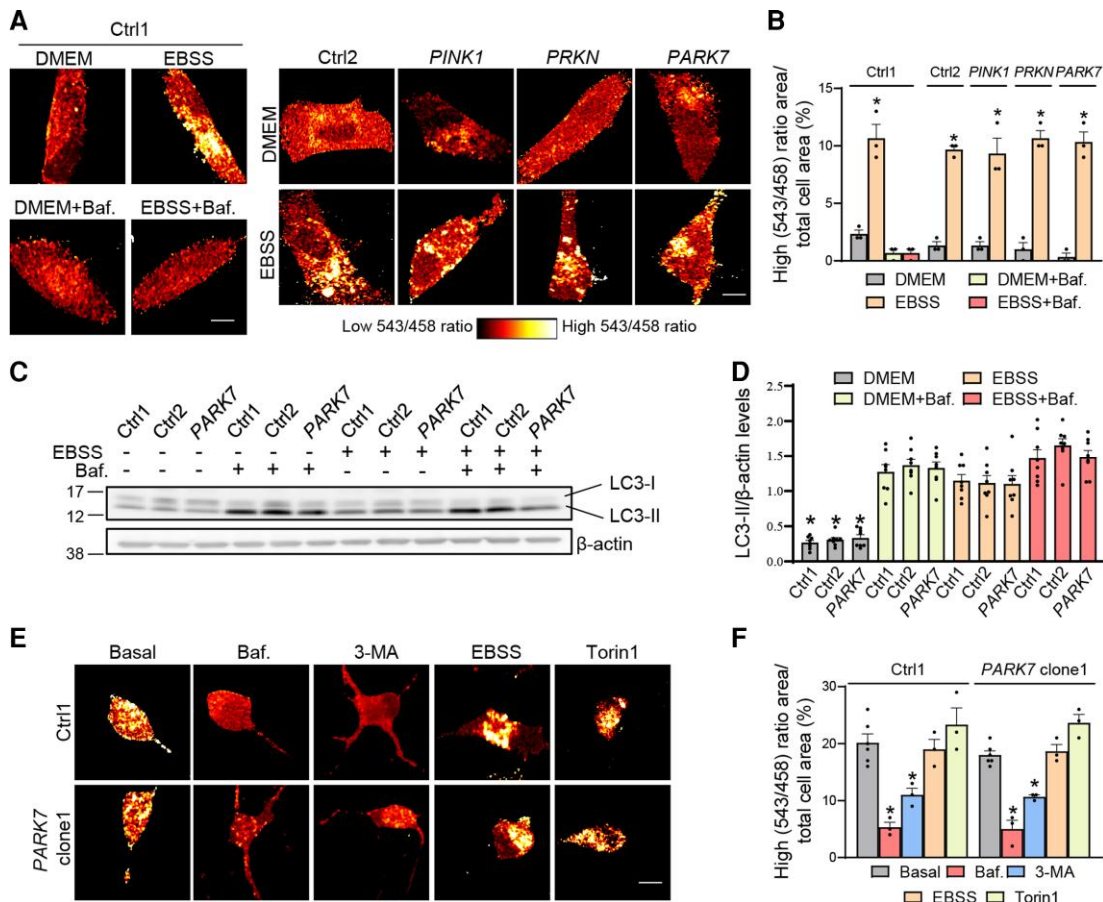
Figure 3 Non-selective autophagy is preserved in *PARK7* mutant fibroblasts and neurons. (**A** and **B**) Fibroblasts from healthy controls (Ctrl1, Ctrl2) and PD patients with homozygous *PINK1*, compound heterozygous *PRKN* or homozygous *PARK7* mutations were transfected with Keima and incubated either in standard culture medium (DMEM) or in EBSS for 4 h to trigger starvation-induced autophagy, in the presence or absence of bafilomycin A1 (Baf., 100 nM), followed by live ratiometric Keima imaging. High (543:458) ratio signal corresponds to Keima present inside lysosomes. (**B**) Quantification ($n = 3$). *$P < 0.0001$ compared with all other conditions in the same subject. (**C** and **D**) Ctrl1 and *PARK7* mutant fibroblasts were incubated for 4 h in DMEM or EBSS in the presence or absence of Baf. (100 nM), followed by WB for LC3. (**D**) Quantification ($n = 8$). *$P < 0.0001$ compared with all other conditions in the same subject. (**E** and **F**) Neurons from Ctrl1 and a PD patient with *PARK7* mutations (clone 1) were transduced with Keima lentivirus and incubated in EBSS for 4 h or treated with the mTOR inhibitor Torin1 (1 μM), Baf. (100 nM) or 3-methyladenine (3-MA, 10 mM) for 24 h, followed by live Keima imaging. (**F**) Quantification ($n = 3$–6). *$P < 0.001$ compared with the basal, EBSS and Torin1 conditions in the same subject. Scale bars = 10 μm.

neurons (Supplementary Fig. 10A and B and Supplementary Videos 1 and 2). Moreover, subcellular fractionation and western blotting revealed that valinomycin treatment of control neurons induced an ~2.5-fold increase in the amount of endogenous optineurin in the mitochondrial fraction, while this translocation was abrogated in *PARK7* mutant neurons (Fig. 6F–I).

Overexpression of wild-type DJ-1 in *PARK7* mutant cells rescued valinomycin-induced mitochondrial optineurin accumulation (Fig. 6B and C and Supplementary Fig. 9B). The optineurin binding partners LC3 (Supplementary Fig. 11) and RAB10[35] (Supplementary Fig. 12) also showed diminished accumulation on depolarized mitochondria in *PARK7* mutant cells.

We previously found that increased phosphorylation of RAB10 at threonine 73 (T73) by mutant LRRK2 impaired translocation of RAB10 and optineurin to depolarized mitochondria.[35] WB with an antibody against RAB10 phosphorylated at T73 showed no difference between *PARK7* mutant and wild-type fibroblasts (Supplementary Fig. 13), indicating that the deficit in RAB10 and optineurin translocation in DJ-1-deficient cells was not due to increased RAB10 phosphorylation.

Phosphorylation of serine residues S473 and S513 of optineurin by activated TANK binding kinase 1 (TBK1) promotes binding of optineurin to ubiquitin chains.[10,42] TBK1 is activated on mitochondrial depolarization in a PINK1/parkin-dependent manner.[10,42] Consistent with previous work,[10,42,43] we found that TBK1 activation, as measured by phosphorylation on its activation loop site S172, was clearly induced by 1 h of valinomycin exposure and declined thereafter (Supplementary Fig. 14A and B). There was no difference in phospho-TBK1[S172]:TBK1 ratios after valinomycin treatment between wild-type and *PARK7* mutant fibroblasts, indicating that DJ-1 deficiency did not interfere with TBK1 activation (Supplementary Fig. 14C and D).

Besides optineurin, the autophagy receptor NDP52 has also been found to mediate PINK1/parkin-dependent mitophagy in some,[8,10] but not all,[44] studies. We found that fibroblasts expressed both optineurin and NDP52 (Supplementary Fig. 15A). To assess potential redundancy of these autophagy receptors,[8,44] we knocked down optineurin with two different siRNAs (Supplementary Fig. 16A and B). Optineurin knockdown drastically reduced valinomycin-induced mitophagy, indicating that NDP52 did not compensate for loss of optineurin in this pathway in this cell type (Supplementary Fig.
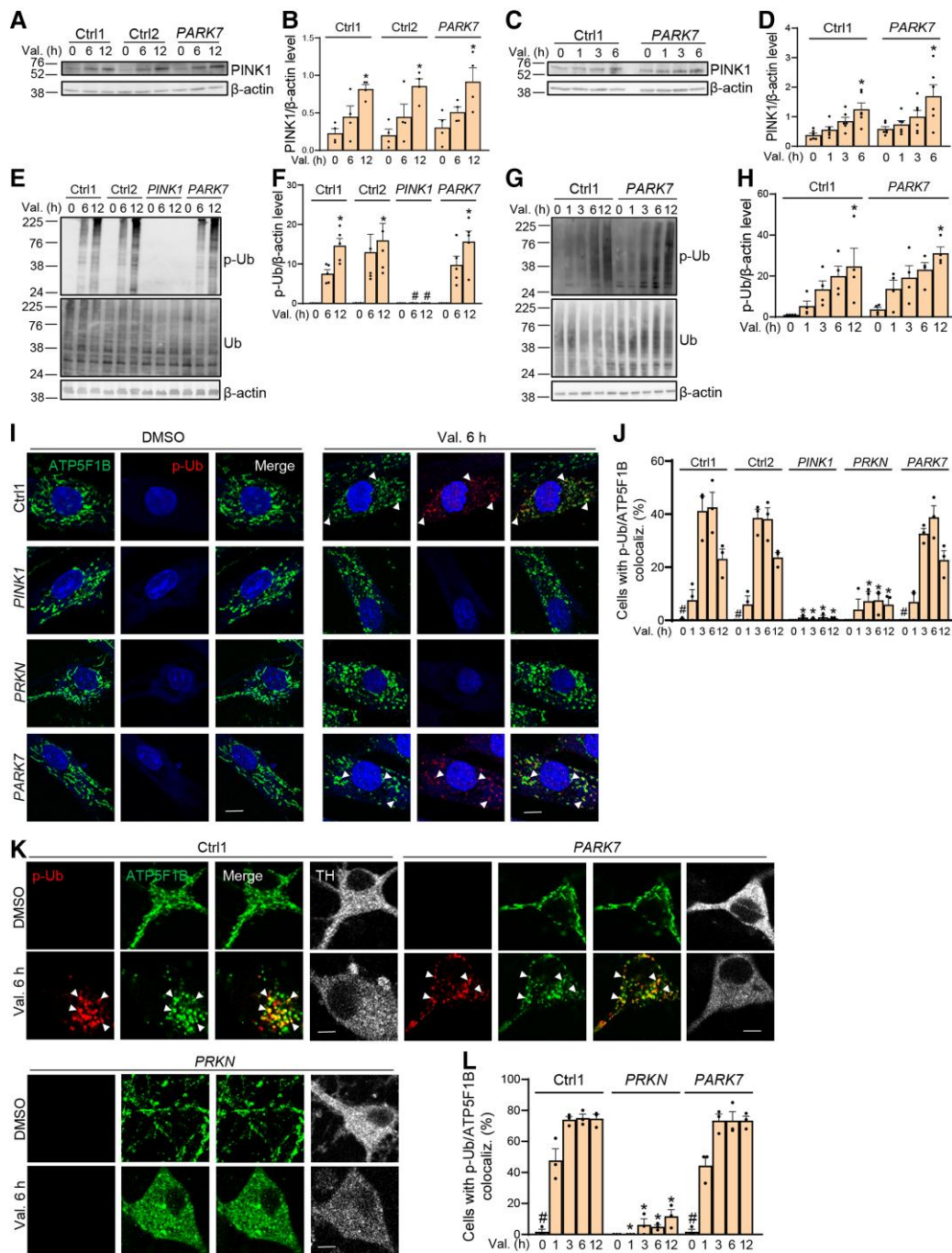
Figure 4 PINK1 accumulation and activity is intact in *PARK7* mutant cells. (**A** and **B**) Healthy control (Ctrl1, Ctrl2) and *PARK7* mutant fibroblasts were treated with valinomycin (Val., 1 µM) for the indicated time, followed by WB for endogenous PINK1. (**B**) Quantification (*n* = 4). *P < 0.05 compared with DMSO in the same subject. (**C** and **D**) Ctrl1 and *PARK7* mutant (clone 1) iPSC-derived neurons were treated with Val. (1 µM) for the indicated time, followed by western for endogenous PINK1. (**D**) Quantification (*n* = 6). *P < 0.05 compared with DMSO in the same subject. (**E** and **F**) Ctrl1, Ctrl2, *PINK1* mutant and *PARK7* mutant fibroblasts were treated with Val., followed by western for endogenous phospho-ubiquitin (p-Ub) and total Ub. (**F**) Quantification (*n* = 4–5). *P < 0.05 compared with DMSO in the same subject. #P < 0.05 compared with Ctrl1, Ctrl2 and *PARK7* after the same duration of Val. exposure. (**G** and **H**) Ctrl1 and *PARK7* mutant (clone 1) neurons were treated with Val. (1 µM) as indicated, followed by western for endogenous p-Ub and total Ub. (**H**) Quantification (*n* = 4). *P < 0.05 compared with DMSO in the same subject. (**I** and **J**) Ctrl1, Ctrl2, *PINK1*, *PRKN* and *PARK7* mutant fibroblasts were treated with DMSO or valinomycin (Val., 1 µM) for the indicated time and immunostained for endogenous phospho-ubiquitin (p-Ub) and the mitochondrial marker ATP5F1B. Nuclei were stained with TOTO-3. Arrowheads in **I** indicate examples of p-Ub puncta that colocalize with mitochondria. (**J**) Quantification of the percentage of cells with p-Ub/ATP5F1B colocalization (*n* = 3). *P < 0.05 compared with Ctrl1, Ctrl2 and *PARK7* after the same duration of Val. exposure. #P < 0.005 compared with Val. 1, 3, 6 and 12 h in the same subject. (**K** and **L**) On day 50 after neuronal induction, Ctrl1, *PRKN* (clone 1) and *PARK7* (clone 1) mutant neurons were treated with DMSO or Val. (1 µM) for the indicated time and immunostained for endogenous p-Ub, ATP5F1B and tyrosine hydroxylase (TH). Arrowheads in **K** indicate examples of p-Ub puncta that colocalize with mitochondria. (**L**) Quantification of the percentage of TH-positive cells with p-Ub/ATP5F1B colocalization (*n* = 3). *P < 0.0001 compared with Ctrl1 and *PARK7* after the same duration of Val. exposure. #P < 0.0001 compared with all Val. conditions in the same subject. Scale bars = 10 µm.
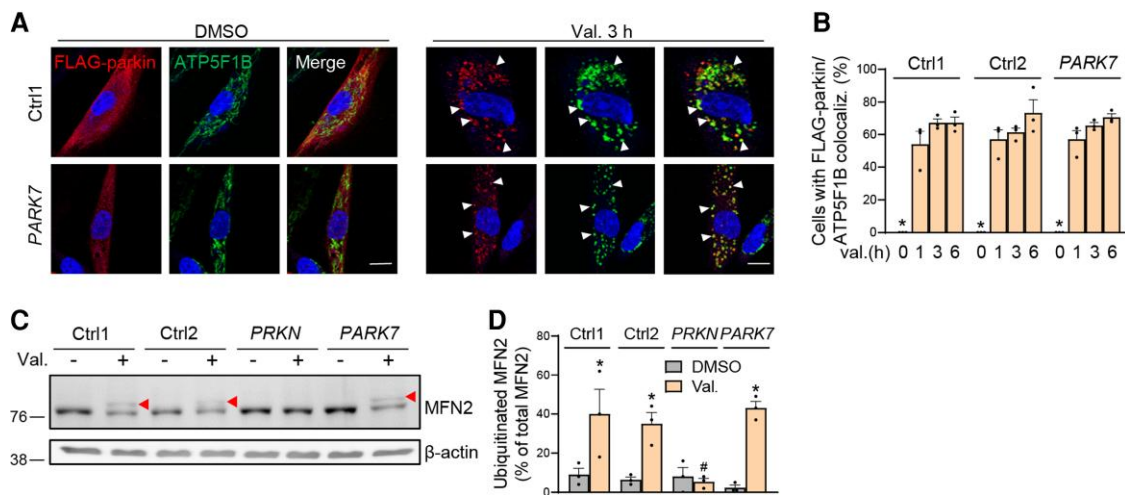
Figure 5 Parkin activation is intact in *PARK7* mutant cells. (**A** and **B**) Control and *PARK7* mutant fibroblasts were transfected with FLAG-parkin. After 24 h cells were treated with DMSO or Val. (1 µM) for the indicated time and immunostained for FLAG and the mitochondrial marker ATP5F1B. Nuclei were stained with TOTO-3. Arrowheads indicate parkin puncta on mitochondria. Scale bar = 10 µm. (**B**) Quantification (*n* = 3). *$P < 0.0001$ compared with all Val. conditions in the same subject. (**C** and **D**) Control, *PRKN* mutant and *PARK7* mutant fibroblasts were treated with DMSO or valinomycin (Val., 1 µM) for 3 h, followed by western for mitofusin 2 (MFN2). Red arrowheads indicate ubiquitinated MFN2. (**D**) Quantification (*n* = 3). *$P < 0.05$ compared with DMSO in the same subject. #$P < 0.05$ compared with Val. in Ctrl1, Ctrl2 and *PARK7*.

16C and D). In brain and human iPSC-derived dopaminergic neurons, NDP52 is not expressed, in contrast to optineurin.[8,11,12] We confirmed with WB that iPSC-derived dopaminergic neuronal cultures strongly expressed optineurin, but not NDP52 (Supplementary Fig. 15B).

DJ-1 translocates with optineurin to depolarized mitochondria in a PINK1/parkin-dependent manner

To better understand the role of DJ-1 in PINK1/parkin-mediated mitophagy, we analysed its subcellular localization. In control fibroblasts and dopaminergic neurons, endogenous DJ-1 was mostly cytosolic in basal conditions (Fig. 7A–D). However, after valinomycin exposure, endogenous DJ-1 showed puncta that strongly colocalized with mitochondria, both in fibroblasts (Fig. 7A and B) and dopaminergic neurons (Fig. 7C and D). This was confirmed for endogenous DJ-1 in neurons by SIM (Supplementary Fig. 10C and D and Supplementary Video 3) and by mitochondrial fractionation and western blotting (Fig. 7E and F).

DJ-1 translocated to depolarized mitochondria with slower kinetics than parkin: DJ-1 did not yet show significant translocation after 1 h of valinomycin exposure (Fig. 7B), whereas parkin translocation at that time point was already nearly maximal (Fig. 5B). However, the translocation time course of DJ-1 closely resembled that of optineurin (Fig. 7B). The mitochondrial DJ-1 puncta after valinomycin treatment strongly colocalized with optineurin (Fig. 7G and H) and also with parkin, phospho-ubiquitin and LC3 (Supplementary Fig. 17).

Overexpressed FLAG-tagged DJ-1[C106A] translocated as efficiently to depolarized mitochondria as wild-type FLAG-tagged DJ-1, indicating that oxidation of C106 was not required for DJ-1 translocation (Supplementary Fig. 18).

To assess whether DJ-1 and optineurin are physically close to each other, we performed *in situ* PLA for the endogenous proteins. A positive PLA signal for two proteins indicates that they are in close proximity (<40 nm distance), typically implying that they are direct or indirect interactors.[45,46] Specificity of the PLA signal was

demonstrated using technical negative controls, in which we omitted either the DJ-1 or the optineurin primary antibody (Supplementary Fig. 19A), as well as biological negative controls, in which we performed PLA for DJ-1 or optineurin and proteins not known to interact with DJ-1 or optineurin (cytosolic protein GTP cyclohydrolase 1, endoplasmic reticulum markers PDI and calnexin, Golgi markers GM-130 and GOLGA5, and early endosome marker EEA1) (Supplementary Fig. 19B). We observed abundant positive PLA signals for endogenous DJ-1 and optineurin, both in basal conditions and after mitochondrial depolarization (Fig. 7I and J). The total number of DJ-1/optineurin PLA dots did not change significantly after mitochondrial depolarization, but the percentage of DJ-1/optineurin PLA dots that colocalized with mitochondria strongly increased after valinomycin exposure (Fig. 7I and J). Taken together, the PLA data indicated that DJ-1 and optineurin were localized in intimate proximity in the cytosol in basal conditions and migrated together to mitochondria after mitochondrial depolarization.

Furthermore, endogenous optineurin coimmunoprecipitated with DJ-1-FLAG in control fibroblasts (Fig. 7K). Mitochondrial depolarization had no significant effect on the interaction between optineurin and DJ-1: after 6 h treatment with valinomycin, the amount of optineurin coimmunoprecipitated with DJ-1-FLAG, divided by the amount of optineurin present in the input, was 98.3 ± 22.1% of the value after DMSO treatment (*n* = 6; $P = 0.94$).

Importantly, translocation of endogenous DJ-1 to depolarized mitochondria was severely impaired in *PINK1* mutant and *PRKN* mutant fibroblasts (Fig. 8A and B) and in *PRKN* mutant dopaminergic neurons (Fig. 8C and D). This was confirmed for endogenous DJ-1 in *PRKN* mutant neurons by SIM (Supplementary Fig. 10C and D and Supplementary Video 4) and by western blotting of mitochondrial fractions (Fig. 8E and F).

Overexpressed DJ-1 also failed to translocate to depolarized mitochondria in *PINK1* and *PRKN* mutant fibroblasts (Supplementary Fig. 20) and did not rescue the mitophagy defect of these cells (Fig. 8G and H). Thus, DJ-1 depends on PINK1 and parkin for its translocation to mitochondria and does not compensate for loss of the upstream effects of PINK1 or parkin in this pathway.
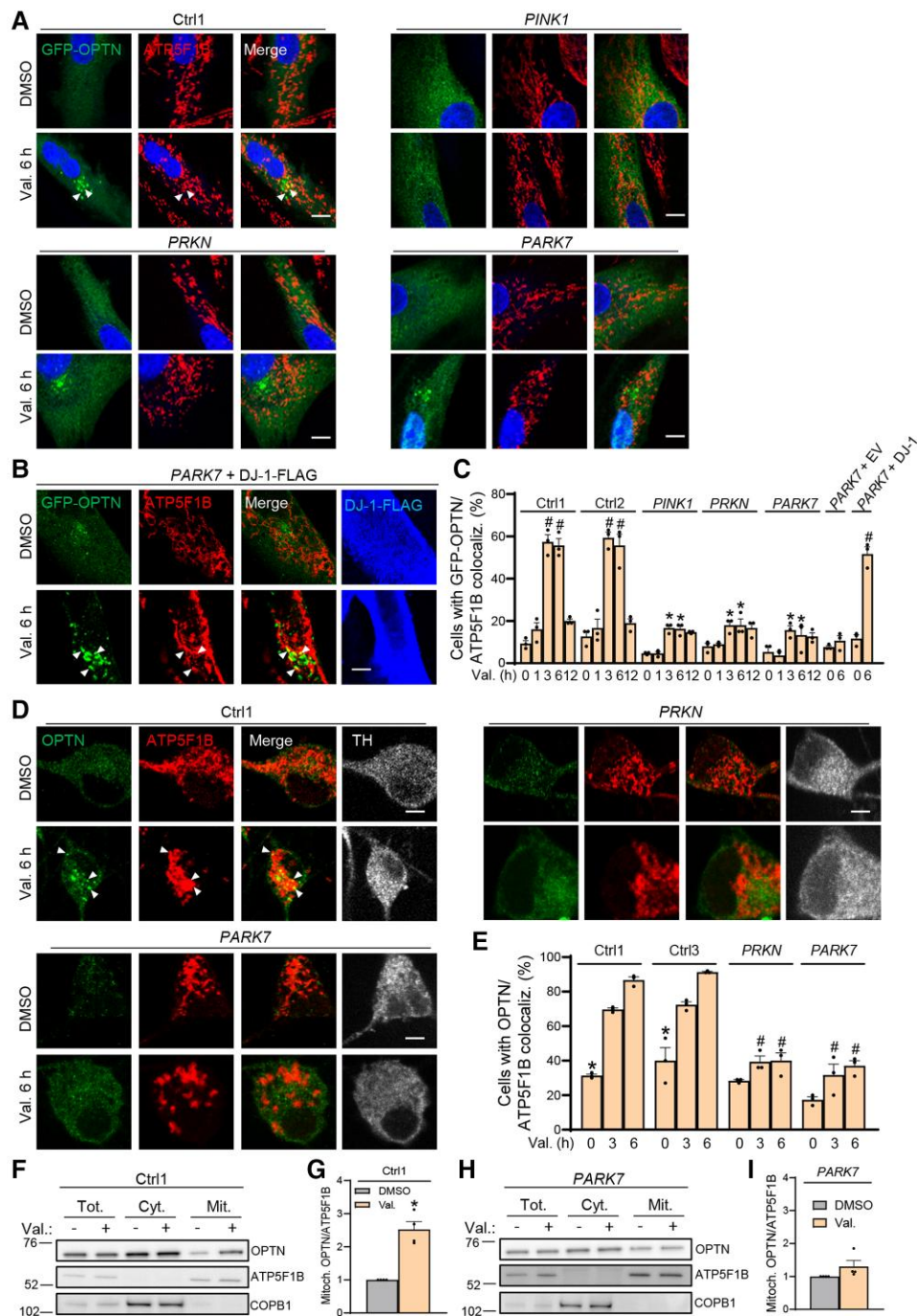
Figure 6 Optineurin recruitment to depolarized mitochondria is impaired in PARK7 mutant fibroblasts and neurons. (**A–C**) Control (Ctrl1, Ctrl2), *PINK1*, *PRKN* and *PARK7* mutant fibroblasts were transfected with GFP-tagged optineurin (GFP-OPTN). (**B** and **C**) *PARK7* mutant fibroblasts were cotransfected with GFP-OPTN and either empty vector (EV) or DJ-1-FLAG. (**A–C**) After 24 h cells were treated with DMSO or valinomycin (Val., 1 μM) for the indicated time, and immunostained for the mitochondrial marker ATP5F1B and FLAG. Nuclei in **A** were stained with TOTO-3. Arrowheads indicate GFP-OPTN puncta on mitochondria. Immunostaining images for Ctrl2 and for *PARK7* + EV are shown in Supplementary Fig. 9A and B , respectively. (**C**) Quantification of the percentage of cells showing GFP-OPTN/ATP5F1B colocalization ($n = 3$). #$P < 0.0001$ compared with DMSO in the same subject. *$P < 0.0001$ compared with Ctrl1, Ctrl2 and *PARK7* + DJ-1 after the same duration of Val. exposure. (**D** and **E**) iPSC-derived control, *PRKN* (clone 1) and *PARK7* (clone 1) mutant neurons were treated with DMSO or Val. (1 μM) for the indicated time and immunostained for endogenous OPTN, ATP5F1B and tyrosine hydroxylase (TH). Arrowheads indicate colocalization of OPTN with mitochondria. (**E**) Quantification of the percentage of TH-positive cells showing OPTN/ATP5F1B colocalization ($n = 3$). *$P < 0.0001$ compared with all Val. conditions in the same subject. #$P < 0.001$ compared with Ctrl1 and Ctrl3 after the same duration of Val. exposure. Scale bars = 10 μm. (**F–I**) Ctrl1 neurons (**F** and **G**) and *PARK7* mutant neurons (**H** and **I**) were treated with DMSO or Val. for 6 h, followed by subcellular fractionation and western blotting of total (Tot.), cytosolic (Cyt.) and mitochondrial (Mit.) fractions for endogenous OPTN, ATP5F1B and the non-mitochondrial protein COPB1. Equal amounts of protein (15 μg) were loaded for all fractions. This amount of 15 μg corresponded to nearly the entire mitochondrial fraction and to only ~5% of the cytosolic fraction, explaining why the ~2.5-fold increase in mitochondrial optineurin after valinomycin treatment in Ctrl1 cells (**F** and **G**) did not result in a visible decrease of optineurin in the cytosolic fraction. (**G** and **I**) Quantification of OPTN/ATP5F1B (normalized to DMSO) in the mitochondrial fraction ($n = 4$). *$P < 0.001$ compared with DMSO (**G**).
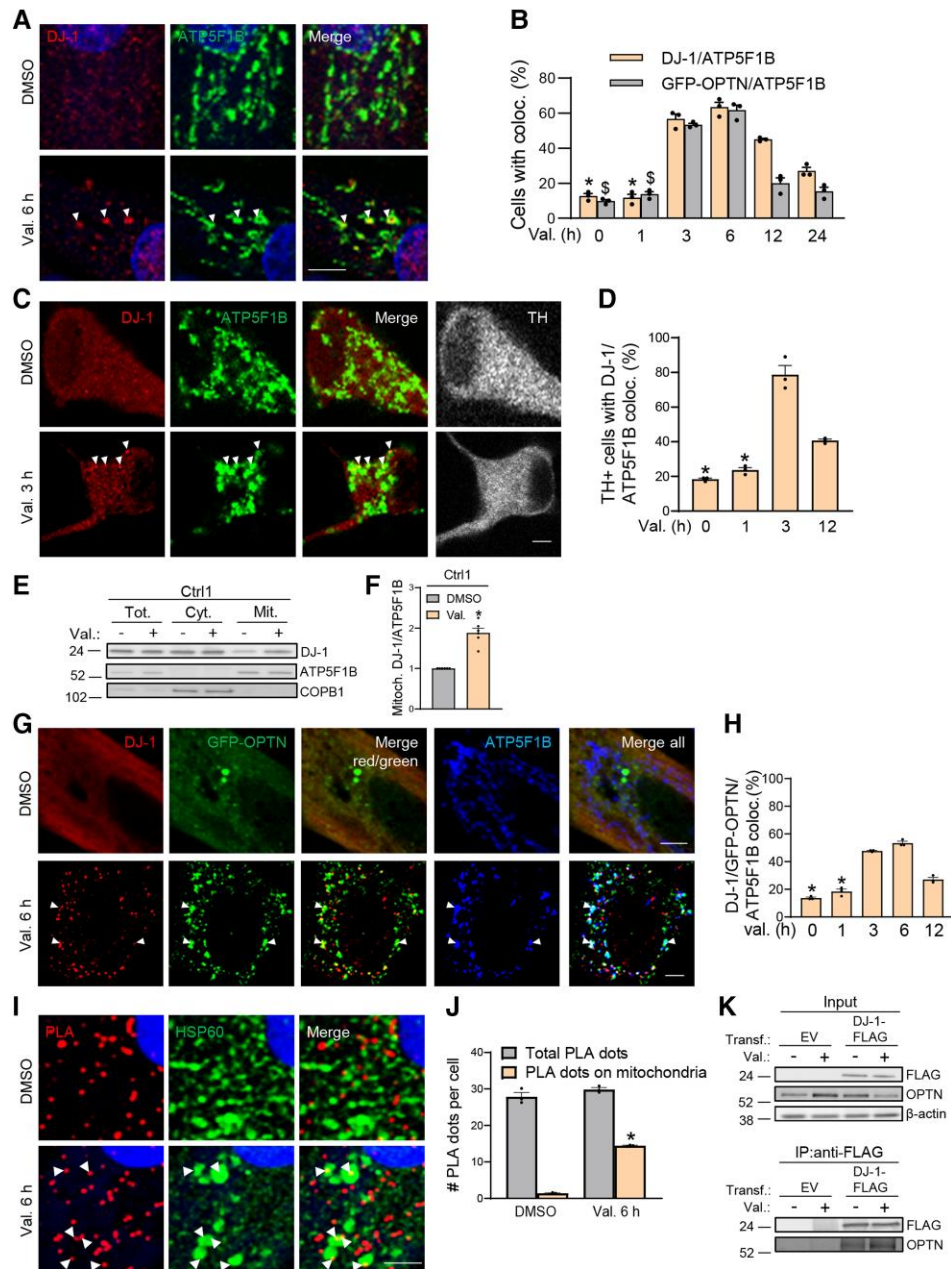
Figure 7 DJ-1 translocates to depolarized mitochondria in close proximity with optineurin in wild-type fibroblasts and neurons. (A and B) Control (Ctrl1) fibroblasts were treated with DMSO or valinomycin (Val., 1 μM) for the indicated time and immunostained for endogenous DJ-1 and the mitochondrial marker ATP5F1B. Nuclei were stained with TOTO-3. Arrowheads indicate examples of DJ-1 puncta that colocalize with mitochondria. (**B**) Quantification of the percentage cells with DJ-1/ATP5F1B colocalization ($n=3$). For comparison, the time course of GFP-optineurin (GFP-OPTN)/ATP5F1B colocalization is also shown ($n=3$). *$P<0.005$ compared with the 3, 6, 12 and 24 h Val. condition for DJ-1/ATP5F1B colocalization. $$P<0.0001$ compared with the 3 and 6 h Val. condition for GFP-OPTN/ATP5F1B colocalization. (**C** and **D**) Ctrl1 neurons were treated with Val. (1 μM) for the indicated time and immunostained for endogenous DJ-1, ATP5F1B and tyrosine hydroxylase (TH). Arrowheads indicate examples of DJ-1 puncta that colocalize with mitochondria. (**D**) Quantification of the percentage of TH-positive cells with DJ-1/ATP5F1B colocalization ($n=3$). *$P<0.05$ compared with the 3 and 12 h Val. condition. (**E** and **F**) Ctrl1 neurons were treated with DMSO or Val. for 6 h, followed by subcellular fractionation and western blotting of total (Tot.), cytosolic (Cyt.) and mitochondrial (Mit.) fractions for endogenous DJ-1, ATP5F1B and the non-mitochondrial protein COPB1. Equal amounts of protein (15 μg) were loaded for all fractions. This amount of 15 μg corresponded to nearly the entire mitochondrial fraction and to only ~5% of the cytosolic fraction, explaining why the ~2-fold increase in mitochondrial DJ-1 after valinomycin treatment in Ctrl1 cells (**E** and **F**) did not result in a visible decrease of DJ-1 in the cytosolic fraction. (**F**) Quantification of DJ-1/ATP5F1B (normalized to DMSO) in the mitochondrial fraction ($n=6$). *$P<0.0001$ compared with DMSO. (**G** and **H**) Ctrl1 fibroblasts were transfected with GFP-OPTN and after 24 h cells were treated with DMSO or Val. (1 μM) for the indicated time and immunostained as indicated. Arrowheads indicate examples of colocalization. (**H**) Percentages were quantified of cells with colocalization of DJ-1/GFP-OPTN/ATP5F1B. *$P<0.0001$ compared with the 3 and 6 h Val. condition. (**I** and **J**) Ctrl1 fibroblasts were treated with DMSO or Val. for 6 h, followed by proximity ligation (PLA) with antibodies against endogenous OPTN and DJ-1 and immunostaining for the mitochondrial marker HSP60. Arrowheads indicate examples of PLA dots that colocalize with mitochondria. (**J**) Quantification ($n=3$). *$P<0.0001$ compared with DMSO. Scale bars = 5 μm. (**K**) Ctrl1 fibroblasts were transfected (Transf.) with empty vector (EV) of FLAG-tagged DJ-1, as indicated, and treated with DMSO or Val. for 6 h. After coimmunoprecipitation with anti-FLAG beads, the input and immunoprecipitate (IP) were analysed by sodium dodecyl-sulphate–polyacrylamide gel electrophoresis and western blotting using the indicated antibodies. The shown example is representative of six experiments.
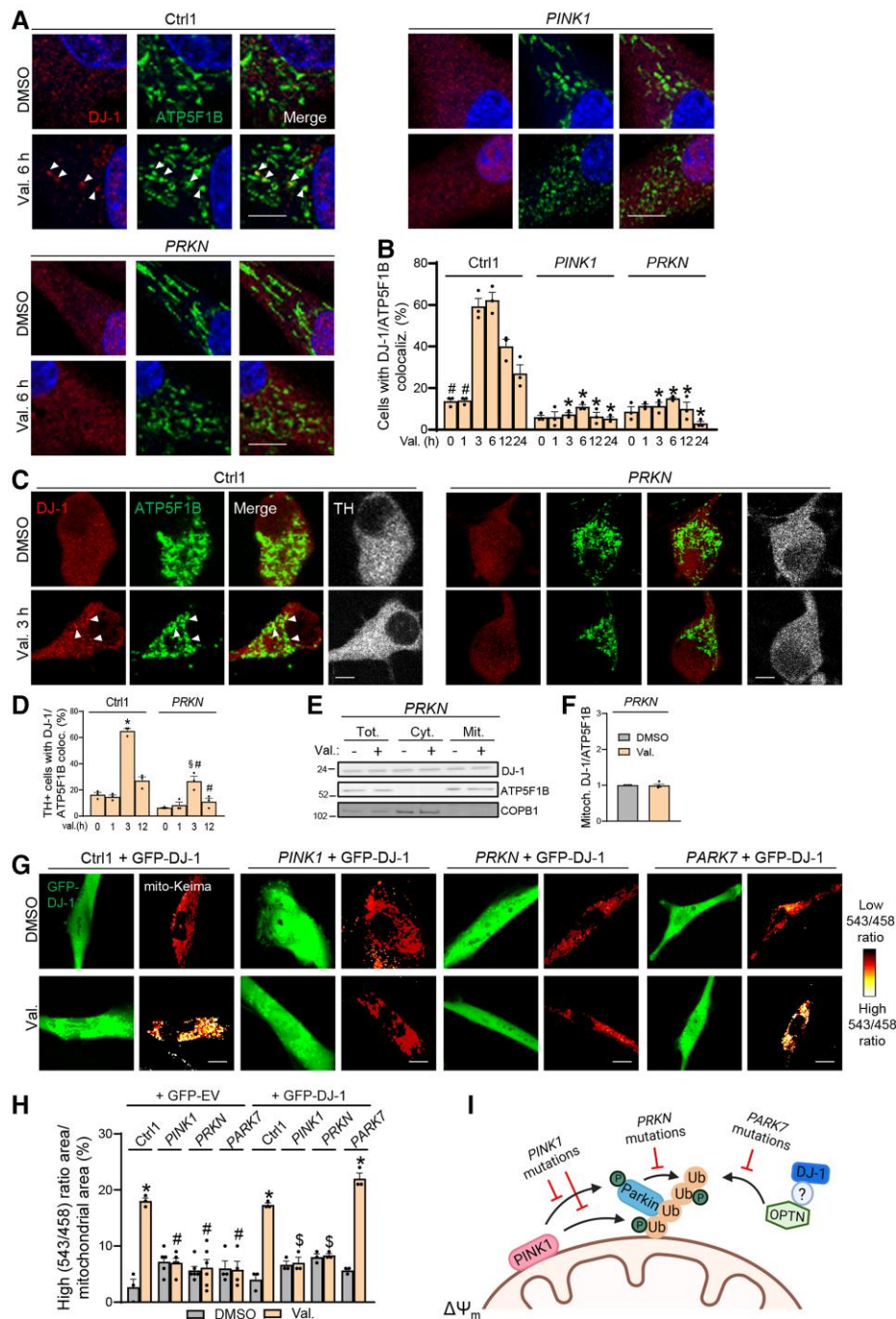
Figure 8 DJ-1 translocation to depolarized mitochondria depends on PINK1 and parkin. (**A** and **B**) Control (Ctrl1), *PINK1* and *PRKN* mutant fibroblasts were treated with DMSO or valinomycin (Val., 1 μM) for the indicated time and immunostained for endogenous DJ-1 and ATP5F1B. Nuclei were stained with TOTO-3. Arrows indicate DJ-1 puncta on mitochondria. (**B**) Quantification ($n = 3$). #$P < 0.05$ compared with the 3, 6, 12 and 24 h Val. conditions in the same subject. *$P < 0.0001$ compared with Ctrl1 after the same duration of Val. exposure. (**C** and **D**) Control (Ctrl1) and *PRKN* mutant (clone 1) neurons were treated with DMSO or Val. (1 μM) for the indicated time and immunostained for endogenous DJ-1, ATP5F1B and tyrosine hydroxylase (TH). Arrowheads indicate DJ-1 puncta that colocalize with mitochondria. (**D**) Quantification ($n = 3$). #$P < 0.005$ compared with Ctrl1 after the same duration of Val. exposure. *$P < 0.0001$ compared with DMSO in the same subject. §$P < 0.001$ compared with DMSO in the same subject. (**E** and **F**) *PRKN* mutant neurons were treated with DMSO or Val. for 6 h, followed by subcellular fractionation and western blotting of total (Tot.), cytosolic (Cyt.) and mitochondrial (Mit.) fractions for endogenous DJ-1, the mitochondrial protein ATP5F1B and the non-mitochondrial protein COPB1. Equal amounts of protein (15 μg) were loaded for all fractions. (**F**) Quantification of DJ-1/ATP5F1B (normalized to DMSO) in the mitochondrial fraction ($n = 4$; $P = 0.92$ for DMSO versus Val.). (**G** and **H**) Ctrl1, *PINK1*, *PRKN* and *PARK7* mutant fibroblasts were transfected with mito-Keima and either GFP empty vector (EV) or GFP-tagged wild-type DJ-1. After 24 h, cells were treated for 48 h with DMSO or Val. (1 μM), followed by live mito-Keima imaging. (**H**) Quantification ($n = 3$). *$P < 0.0001$ compared with DMSO in the same subject. #$P < 0.0001$ compared with Val. in Ctrl1 + GFP-EV. $$P < 0.001$ compared with Val. in Ctrl1 + GFP-*DJ-1* and with Val. in *PARK7* + GFP-DJ-1. Scale bars = 10 μm. (**I**) Model (drawn with Biorender.com). After mitochondrial depolarization PINK1 activates parkin by phosphorylating ubiquitin and parkin. Activated parkin catalyses formation of ubiquitin (Ub) chains on mitochondria. DJ-1 facilitates recruitment of optineurin (OPTN) to mitochondrial ubiquitin chains and interacts with OPTN either directly or indirectly via an unknown (indicated by ?) binding partner. *PINK1*, *PRKN* and *PARK7* mutations interfere with three successive steps in the pathway. P = phosphate; $\Delta\Psi_m$ = mitochondrial depolarization.

Overexpression of parkin is known to strongly increase ubiquitination and clearance of depolarized mitochondria in various cell types.[34,47] Parkin overexpression also enhanced valinomycin-induced mitophagy in *PARK7* mutant fibroblasts (Supplementary Figs 21 and 22). However, valinomycin induced much less mitophagy in parkin-overexpressing *PARK7* mutant fibroblasts than in parkin-overexpressing wild-type fibroblasts, indicating that DJ-1 deficiency negatively affected mitophagy even under conditions of parkin overexpression (Supplementary Figs 21 and 22). Similarly, valinomycin-induced optineurin recruitment to mitochondria was severely reduced in parkin-overexpressing *PARK7* mutant fibroblasts compared to parkin-overexpressing wild-type fibroblasts (Supplementary Fig. 23).

Finally, we wondered whether artificial targeting of DJ-1 to the OMM would be sufficient to recruit optineurin to mitochondria. We fused the N-terminal transmembrane segment (amino acids 1-49) of the OMM protein TOMM20 to DJ-1 carrying a C-terminal FLAG tag (OMM-DJ-1-FLAG). Immunostaining and confocal imaging of transfected control fibroblasts showed that OMM-DJ-1-FLAG strongly colocalized with mitochondria, in contrast to the diffuse cytosolic distribution of DJ-1-FLAG (Supplementary Fig. 24A). This was confirmed by SIM (Supplementary Fig. 24B and C). Subcellular fractionation followed by western blotting also confirmed that OMM-DJ-1-FLAG was predominantly mitochondrial and DJ-1-FLAG mostly cytosolic (Supplementary Fig. 24D). Interestingly, expression of OMM-DJ-1-FLAG induced optineurin recruitment to mitochondria in the absence of valinomycin treatment in control fibroblasts and even in *PINK1* and *PRKN* mutant cells, as shown by confocal imaging (Supplementary Fig. 24E and F) and by SIM (Supplementary Fig. 24G and H). Thus, DJ-1 artificially anchored to the OMM was able to recruit optineurin to mitochondria independently of PINK1/parkin pathway activation.

Discussion

PRKN, *PINK1* and *PARK7* have been unequivocally identified as causative genes for autosomal recessive early-onset PD. *PARK7* mutations are the rarest known cause of recessive PD, accounting for only ~0.4% of early-onset PD cases.[16] Mechanistic studies in cells from PD patients with *PARK7* mutations have been scarce,[29,48,49] probably due to the rarity of these mutations, and the pathogenic mechanisms of DJ-1 deficiency remain poorly understood. In the present study, we demonstrate in patient-derived fibroblasts and neurons that endogenous DJ-1 is essential for PINK1/parkin-mediated mitophagy. Loss of DJ-1 does not impair PINK1 or parkin activation, but blocks mitophagy further downstream at the level of mitochondrial recruitment of optineurin. These findings position DJ-1 downstream of PINK1 and parkin in the same pathway (Fig. 8I) and suggest closely related pathogenic mechanisms for the different forms of autosomal recessive PD.

We found that endogenous DJ-1 translocated from the cytosol to depolarized mitochondria in primary human fibroblasts and dopaminergic neurons. Two previous studies showed that DJ-1 can relocate to mitochondria after exposure to the oxidants H_2O_2 or paraquat in neuroblastoma cell lines.[39,50] One of these studies reported that oxidant-induced mitochondrial translocation of DJ-1 was driven by oxidation of C106[39] while the other study found that mutating C106 had no effect on DJ-1 translocation.[50] In our current study, depolarization-induced mitochondrial translocation of DJ-1 did not require C106 oxidation, but, importantly, depended on PINK1 and parkin.

Our data reveal a close spatial and functional relationship of DJ-1 with optineurin. *In situ* PLA showed intimate proximity of endogenous DJ-1 and optineurin in the cytosol in basal conditions as well as on mitochondria after depolarization. Interestingly, a recent study using APEX2 proximity proteomics, a strategy for unbiased identification of proteins present within 20 nm of a bait protein, identified DJ-1 as a proximity partner of optineurin, but not of other autophagy receptors, further supporting the idea that DJ-1 and optineurin are closely adjacent.[51] Furthermore, we were able to coimmunoprecipitate optineurin with DJ-1-FLAG, suggesting that optineurin and DJ-1 are direct or indirect binding partners. DJ-1 and optineurin translocated to depolarized mitochondria with similar kinetics, and more slowly than parkin. Moreover, optineurin accumulation on damaged mitochondria was abrogated in DJ-1-deficient fibroblasts and dopaminergic neurons, indicating a critical role for DJ-1 in mitochondrial optineurin recruitment. By contrast, non-selective autophagy, which does not require optineurin or other autophagy receptors, was preserved in *PARK7* mutant fibroblasts and neurons. DJ-1 artificially anchored to the OMM enhanced mitochondrial localization of optineurin independently of PINK1/parkin activation, providing further evidence that mitochondrial translocation of DJ-1 contributed to mitochondrial optineurin recruitment.

Optineurin and NDP52 are the main selective autophagy receptors involved in PINK1/parkin-mediated mitophagy.[8] We confirmed the previous finding that optineurin is expressed in neurons, unlike NDP52.[8,11,12] Optineurin is a scaffold protein that drives selective autophagy through interaction with multiple partners.[52] In addition to linking ubiquitinated cargo to autophagosomal membranes via binding to ubiquitin and LC3, optineurin also promotes local phagophore biogenesis via recruitment of ULK1 and ATG9.[8,53] The optineurin complex appears to be a hotspot for mutations causative of neurodegeneration. Mutations in the genes for optineurin and its interactor TBK1 cause amyotrophic lateral sclerosis (ALS) and frontotemporal dementia.[54] Interestingly, although most patients with *PARK7* mutations have typical early-onset PD, some develop ALS and dementia in addition to parkinsonism.[55,56] PD-linked *LRRK2* mutations also interfere with mitochondrial optineurin accumulation during PINK1/parkin-mediated mitophagy.[35] In wild-type cells, the LRRK2 substrate RAB10 binds with optineurin and promotes optineurin accumulation on depolarized mitochondria. Pathogenic *LRRK2* mutations enhance phosphorylation of RAB10 at T73, which disrupts RAB10 interaction with optineurin and mitochondrial optineurin recruitment.[35] Here, we found no change in RAB10 T73 phosphorylation levels in DJ-1-deficient cells compared with wild-type, indicating that *PARK7* and *LRRK2* mutations interfere with mitochondrial optineurin recruitment via different mechanisms. Future studies will need to further unravel how DJ-1 facilitates optineurin recruitment to damaged mitochondria.

The essential role for DJ-1 in PINK1/parkin-dependent mitochondrial quality control may explain several previous observations in DJ-1-deficient cells, such as their reduced average mitochondrial membrane potential,[29,30,57] increased mitochondrial fragmentation[29,30,49] and elevated mitochondrial ROS production.[29,48,57] DJ-1-mediated removal of dysfunctional mitochondria probably contributes to the ability of DJ-1 to reduce oxidative stress, along with other reported mechanisms such as direct ROS scavenging by DJ-1 via C106 oxidation[20] and DJ-1-induced activation of Nrf2, a regulator of anti-oxidant transcriptional responses.[58]

In HeLa cells, DJ-1 overexpression did not rescue the mitochondrial morphological phenotype caused by *PINK1* knockdown.[59] In *Drosophila*, one study found that DJ-1 ameliorated the phenotype

of *pink1* mutant, but not *parkin* mutant flies,[60] while another study found no rescuing effect of DJ-1 in *pink1* deficient flies.[61] In the current study, we found that DJ-1 did not rescue the mitophagy defect of *PINK1* or *PRKN* mutant fibroblasts, indicating that DJ-1 cannot compensate for loss of the kinase activity of PINK1 or the E3 ubiquitin ligase activity of parkin that occur upstream in this pathway.

A limitation of our study is that we did not use isogenic control fibroblasts or neurons. However, overexpression of DJ-1 rescued mitophagy in *PARK7* mutant fibroblasts and neurons, and siRNA-mediated DJ-1 knockdown induced a mitophagy defect in fibroblasts from healthy controls, indicating that the mitophagy defect in *PARK7* mutant cells was indeed due to loss of DJ-1.

In conclusion, we show that DJ-1 is an essential downstream mediator in PINK1/parkin-dependent mitophagy. On the basis of this, we propose that disruption of PINK1/parkin/DJ-1-mediated mitophagy may be a common pathogenic mechanism in autosomal recessive PD. This convergence further enhances the attractiveness of this pathway as a target for disease modification for autosomal recessive and early-onset PD.

Acknowledgements

Funding

Competing interests

The authors report no competing interests.

Supplementary material

Supplementary material is available at *Brain* online.

References

1. GBD 2016 Parkinson's Disease Collaborators. Global, regional and national burden of Parkinson's disease. 2016. 1990-2016: A systematic analysis for the global burden of disease study 2016. *Lancet Neurol*. 2018;17:939-53.
2. Poewe W, Seppi K, Tanner CM, *et al*. Parkinson disease. *Nat Rev Dis Primers*. 2017;3:17013.
3. Bandres-Ciga S, Diez-Fairen M, Kim JJ, Singleton AB. Genetics of Parkinson's disease: An introspection of its journey towards precision medicine. *Neurobiol Dis*. 2020;137:104782.
4. Wittke C, Petkovic S, Dobricic V, *et al*. Genotype-phenotype relations for the atypical parkinsonism genes: MDSGene systematic review. *Mov Disord*. 2021;36:1499-110.
5. Malpartida AB, Williamson M, Narendra DP, Wade-Martins R, Ryan BJ. Mitochondrial dysfunction and mitophagy in Parkinson's disease: From mechanism to therapy. *Trends Biochem Sci*. 2021;46:329-43.
6. Pickrell AM, Youle RJ. The roles of PINK1, parkin, and mitochondrial fidelity in Parkinson's disease. *Neuron*. 2015;85:257-73.
7. Yamano K, Matsuda N, Tanaka K. The ubiquitin signal and autophagy: An orchestrated dance leading to mitochondrial degradation. *EMBO Rep*. 2016;17:300-16.
8. Lazarou M, Sliter DA, Kane LA, *et al*. The ubiquitin kinase PINK1 recruits autophagy receptors to induce mitophagy. *Nature*. 2015;524:309-14.
9. Wong YC, Holzbaur EL. Optineurin is an autophagy receptor for damaged mitochondria in parkin-mediated mitophagy that is disrupted by an ALS-linked mutation. *Proc Natl Acad Sci USA*. 2014;111:E4439-48.
10. Heo JM, Ordureau A, Paulo JA, Rinehart J, Harper JW. The PINK1-PARKIN mitochondrial ubiquitylation pathway drives a program of OPTN/NDP52 recruitment and TBK1 activation to promote mitophagy. *Mol Cell*. 2015;60:7-20.
11. Korioth F, Gieffers C, Maul GG, Frey J. Molecular characterization of NDP52, a novel protein of the nuclear domain 10, which is redistributed upon virus infection and interferon treatment. *J Cell Biol*. 1995;130:1-13.
12. Shiba-Fukushima K, Ishikawa KI, Inoshita T, *et al*. Evidence that phosphorylated ubiquitin signaling is involved in the etiology of Parkinson's disease. *Hum Mol Genet*. 2017;26:3172-85.
13. Mouton-Liger F, Jacoupy M, Corvol JC, Corti O. PINK1/Parkin-dependent Mitochondrial surveillance: From pleiotropy to Parkinson's disease. *Front Mol Neurosci*. 2017;10:120.
14. Pollock L, Jardine J, Urbé S, Clague MJ. The PINK1 repertoire: Not just a one trick pony. *Bioessays*. 2021;43:e2100168.
15. Bonifati V, Rizzu P, van Baren MJ, *et al*. Mutations in the DJ-1 gene associated with autosomal recessive early-onset parkinsonism. *Science*. 2003;299:256-9.
16. Kilarski LL, Pearson JP, Newsway V, *et al*. Systematic review and UK-based study of PARK2 (parkin), PINK1, PARK7 (DJ-1) and LRRK2 in early-onset Parkinson's disease. *Mov Disord*. 2012;27:1522-9.
17. Mencke P, Boussaad I, Romano CD, Kitami T, Linster CL, Krüger R. The role of DJ-1 in cellular metabolism and pathophysiological implications for Parkinson's disease. *Cells*. 2021;10:347.
18. Xu J, Zhong N, Wang H, *et al*. The Parkinson's disease-associated DJ-1 protein is a transcriptional co-activator that protects against neuronal apoptosis. *Hum Mol Genet*. 2005;14:1231-41.
19. Andres-Mateos E, Perier C, Zhang L, *et al*. DJ-1 gene deletion reveals that DJ-1 is an atypical peroxiredoxin-like peroxidase. *Proc Natl Acad Sci USA*. 2007;104:14807-12.
20. Taira T, Saito Y, Niki T, Iguchi-Ariga SMM, Takahashi K, Ariga H. DJ-1 has a role in antioxidative stress to prevent cell death. *EMBO Rep*. 2004;5:213-8.
21. Jun YW, Kool ET. Small substrate or large? Debate over the mechanism of glycation adduct repair by DJ 1. *Cell Chem Biol*. 2020;27:1117-23.
22. Chen J, Li L, Chin LS. Parkinson disease protein DJ-1 converts from a zymogen to a protease by carboxyl-terminal cleavage. *Hum Mol Genet*. 2010;19:2395-408.
23. Matsuda N, Kimura M, Queliconi BB, *et al*. Parkinson's disease-related DJ-1 functions in thiol quality control against aldehyde attack in vitro. *Sci Rep*. 2017;7:12816.
24. Moscovitz O, Ben-Nissan G, Fainer I, Pollack D, Mizrachi L, Sharon M. The Parkinson's-associated protein DJ-1 regulates the 20S proteasome. *Nat Commun*. 2015;6:6609.
25. Schendelman S, Jonason A, Martinat C, Leete T, Abeliovich A. DJ-1 is a redox-dependent molecular chaperone that inhibits alpha-synuclein aggregate formation. *PLoS Biol*. 2004;2:e362.

26. Piston D, Alvarez-Erviti L, Bansal V, *et al*. DJ-1 is a redox sensitive adapter protein for high molecular weight complexes involved in regulation of catecholamine homeostasis. *Hum Mol Genet*. 2017;26:4028-41.

27. Kyung JW, Kim JM, Lee W, *et al*. DJ-1 deficiency impairs synaptic vesicle endocytosis and reavailability at nerve terminals. *Proc Natl Acad Sci USA*. 2018;115:1629-34.

28. Van der Brug MP, Blackinton J, Chandran J, *et al*. RNA Binding activity of the recessive parkinsonism protein DJ-1 supports involvement in multiple cellular pathways. *Proc Natl Acad Sci USA*. 2008;105:10244-9.

29. Krebiehl G, Ruckerbauer S, Burbulla LF, *et al*. Reduced basal autophagy and impaired mitochondrial dynamics due to loss of Parkinson's disease-associated protein DJ-1. *PLoS ONE*. 2010;5:e9367.

30. Thomas KJ, McCoy MK, Blackinton J, *et al*. DJ-1 acts in parallel to the PINK1-parkin pathway to control mitochondrial function and autophagy. *Hum Mol Genet*. 2011;20:40-50.

31. Van Humbeeck C, Cornelissen T, Hofkens H, *et al*. Parkin interacts with Ambra1 to induce mitophagy. *J Neurosci*. 2011;31:10249-61.

32. Katayama H, Kogure T, Mizushima N, Yoshimori T, Miyawaki A. A sensitive and quantitative technique for detecting autophagic events based on lysosomal delivery. *Chem Biol*. 2011;18:1042-52.

33. Delva A, Race V, Boon E, Van Laere K, Vandenberghe W. Parkinson's disease with a homozygous *PARK7* mutation and clinical onset at the age of 5 years. *Mov Disord Clin Pract*. 2020;8:149-52.

34. Cornelissen T, Haddad D, Wauters F, *et al*. The deubiquitinase USP15 antagonizes parkin-mediated mitochondrial ubiquitination and mitophagy. *Hum Mol Genet*. 2014; 23:5227-42.

35. Wauters F, Cornelissen T, Imberechts D, *et al*. *LRRK2* Mutations impair depolarization-induced mitophagy through inhibition of mitochondrial accumulation of RAB10. *Autophagy*. 2020;16:203-22.

36. Takahashi K, Tababe K, Ohnuki M, *et al*. Induction of pluripotent stem cells from adult human fibroblasts by defined factors. *Cell*. 2007;131:861-72.

37. Kriks S, Shim JW, Piao J, *et al*. Dopamine neurons derived from human ES cells efficiently engraft in animal models of Parkinson's disease. *Nature*. 2011;480:547-51.

38. Rannikko EH, Vesterager LB, Shaik JH, *et al*. Loss of DJ-1 protein stability and cytoprotective function by Parkinson's disease-associated proline-158 deletion. *J Neurochem*. 2013;125:314-27.

39. Canet-Aviles RM, Wilson MA, Miller DW, *et al*. The Parkinson's disease protein DJ-1 is neuroprotective due to cysteine-sulfinic acid-driven mitochondrial localization. *Proc Natl Acad Sci USA*. 2004;101:9103-8.

40. Mizushima N, Komatsu M. Autophagy: renovation of cells and tissues. *Cell*. 2011;147:728-41.

41. Maday S, Holzbaur EL. Compartment-specific regulation of autophagy in primary neurons. *J Neurosci*. 2016;36:5933-45.

42. Richter B, Sliter DA, Herhaus L, *et al*. Phosphorylation of OPTN by TBK1 enhances its binding to Ub chains and promotes selective autophagy of damaged mitochondria. *Proc Natl Acad Sci USA*. 2016;113:4039-44.

43. Hung CM, Lombardo PS, Malik N, *et al*. AMPK/ULK1-mediated phosphorylation of parkin ACT domain mediates an early step in mitophagy. *Sci Adv*. 2021;7:eabg4544.

44. Moore AS, Holzbaur EL. Dynamic recruitment and activation of ALS-associated TBK1 with its target optineurin are required for efficient mitophagy. *Proc Natl Acad Sci USA*. 2016;113:E3349-E3358.

45. Alam MS. Proximity ligation assay (PLA). *Methods Mol Biol*. 2022; 2422:191-201.

46. Söderberg O, Gullberg M, Jarvius M, *et al*. Direct observation of individual endogenous protein complexes in situ by proximity ligation. *Nat Methods*. 2006;3:995-1000.

47. Geisler S, Holmström KM, Skujat D, *et al*. PINK1/Parkin-mediated mitophagy is dependent on VDAC1 and p62/SQSTM1. *Nat Cell Biol*. 2010;12:119-31.

48. Burbulla LF, Song P, Mazzulli JR, *et al*. Dopamine oxidation mediates mitochondrial and lysosomal dysfunction in Parkinson's disease. *Science*. 2017;357:1255-61.

49. Irrcher I, Aleyasin H, Seifert EL, *et al*. Loss of the Parkinson's disease-linked gene DJ-1 perturbs mitochondrial dynamics. *Hum Mol Genet*. 2010; 19:3734-46.

50. Junn E, Jang WH, Zhao X, Jeong BS, Mouradian MM. Mitochondrial localization of DJ-1 leads to enhanced neuroprotection. *J Neurosci Res*. 2009;87:123-9.

51. Zellner S, Schifferer M, Behrends C. Systematically defining selective autophagy receptor-specific cargo using autophagosome content profiling. *Mol Cell*. 2021;81:1337-54.e8.

52. Qiu Y, Wang J, Li H, *et al*. Emerging views of OPTN (optineurin) function in the autophagic process associated with disease. *Autophagy*. 2021;13:1-13.

53. Yamano K, Kikuchi R, Kojima W, *et al*. Critical role of mitochondrial ubiquitination and the OPTN-ATG9A axis in mitophagy. *J Cell Biol*. 2020;219:e201912144.

54. Chua JP, De Calbiac H, Kabashi E, Barmada SJ. Autophagy and ALS: Mechanistic insights and therapeutic implications. *Autophagy*. 2021;18:254-82.

55. Annesi G, Savettieri G, Pugliese P, *et al*. DJ-1 mutations and parkinsonism-dementia-amyotrophic lateral sclerosis complex. *Ann Neurol*. 2005;58:803-7.

56. Hanagasi HA, Giri A, Kartal E, *et al*. A novel homozygous DJ1 mutation causes parkinsonism and ALS in a Turkish family. *Parkinsonism Relat Disord*. 2016;29:117-20.

57. Giaime E, Yamaguchi H, Gautier CA, Kitada T, Shen J. Loss of DJ-1 does not affect mitochondrial respiration but increases ROS production and mitochondrial permeability transition pore opening. *PLoS ONE*. 2012;7:e40501.

58. Clements CM, McNally RS, Conti BJ, Mak TW, Ting JP. DJ-1, a cancer- and Parkinson's disease associated protein, stabilizes the antioxidant transcriptional master regulator Nrf2. *Proc Natl Acad Sci USA*. 2006;103:15091-6.

59. Exner N, Treske B, Paquet D, *et al*. Loss-of-function of human PINK1 results in mitochondrial pathology and can be rescued by parkin. *J Neurosci*. 2007;27:12413-8.

60. Hao LY, Giasson BI, Bonini NM. DJ-1 is critical for mitochondrial function and rescues PINK1 loss of function. *Proc Natl Acad Sci USA*. 2010;107:9747-52.

61. Yang Y, Gehrke S, Imai Y, *et al*. Mitochondrial pathology and muscle and dopaminergic neuron degeneration caused by inactivation of *Drosophila* Pink1 is rescued by parkin. *Proc Natl Acad Sci USA*. 2006;103:10793-8.